Discretization of a hybrid model for acoustic wave propagation in layered fluid media*

ELENA SUNDKVIST AND KURT OTTO†

Abstract

The objective is to construct and discretize (to fourth-order accuracy) a hybrid model for waveguide problems, where a finite difference method for inhomogeneous layers is coupled to a boundary element method (BEM) for a set of homogeneous layers. Such a hybrid model is adequate for underwater acoustics in complicated environments. Waveguides with either plane or axial symmetry are treated, which leads to (algebraically) two-dimensional problems. The main focus is on the collocated BEM.

1 Introduction

The Helmholtz equation describes wave propagation in applications such as acoustics [8] and electromagnetics [19]. For underwater acoustics in complicated environments concerning, e.g., submarine applications in the Swedish archipelago, it is relevant to model time-harmonic sound propagation in (two-dimensional) waveguides consisting of water, soft sediment, hard sediment or bedrock layers. The typical situation for such applications is that the sound speed profile is measured for the water layer, whereas only the geometry and the media parameters are estimated for the sediment and bedrock layers. This means that in practice, the feasible model of the waveguide consists of an inhomogeneous water layer followed by various homogeneous sediment or bedrock layers. From a submarine engineering perspective, it is also of considerably *less* interest to compute the sound field for the sediment and bedrock layers than for the water layer. However, the bottom layers afffect the sound field in the water layer, so their effect should not be ignored.

Otto and Larsson have previously constructed a flexible HELM (Helmholtz Equation for Layered Media) solver. It can handle two-dimensional restrictions (plane

*Published electronically June 22, 2011; updated July 31, 2011.

†Department of Information Technology, Uppsala University, Box 337, SE-751 05 Uppsala, Sweden (kurt@it.uu.se).

or axial symmetry) of a smoothly varying bathymetry, real or complex wavenumbers, variable material properties, and layered media. The HELM solver is a generalization and comprehensive revision of the prototype FD4HE [13]. The ingredients of the solution method are fourth-order accurate finite difference [15] and finite element discretizations, domain decomposition [12], and preconditioned Krylov subspace methods. Even though the memory requirements are low, and the gain in arithmetic complexity compared with standard solution methods is large, the finite difference technique has some intrinsic inadequacy. Employing a finite difference (or finite element) discretization of the *differential* formulation of the Helmholtz equation for a waveguide problem of the type above would inevitably introduce a large number of undesired degrees of freedom, since the *interior* of every sediment and bedrock layer is discretized through its grid. This severe disadvantage could be avoided by discretizing the *boundary integral* formulation of the Helmholtz equation for those layers where the interior sound field is of no primary interest. The gist of that approach is to decrease the number of degrees of freedom by discretizing only where the solution is required, and thereby aiming at a reduction of the memory requirements.

The objective of this work is to construct and discretize (to fourth-order accuracy) a hybrid model for waveguide problems, where a finite difference method (like HELM) for inhomogeneous layers is coupled to a boundary element method (BEM) [22] for a set of homogeneous layers. The main focus is on BEM, which has not been applied much to waveguide problems but is well established for scattering problems [7, and the references therein].

The report is organized as follows. In Section 2, both the differential and the boundary integral formulations are stated, and the physical boundary and interface conditions are described. The radiation boundary conditions required at the near- and far-field open boundaries of the waveguide are developed in Section 3. Sections 4 and 5 contain a refined specification of the differential and boundary integral equations and how they are coupled. The discretization is set up in Section 6, which ends with a specification of the linear system of equations that arises. The last section concerns the assembly of the coefficient tensor and the right-hand side. The report ends with two appendices, where subappendix A.2 has a focus on special integration techniques required for the singular integrands arising.

2 Physical problem and governing equations

We model time-harmonic sound wave propagation under water. A waveguide consisting of N fluid layers with different densities and sound speeds is considered. The top n layers (see Fig. 1) are allowed to be acoustically inhomogeneous and the remaining layers are homogeneous. The waves are governed by the Helmholtz

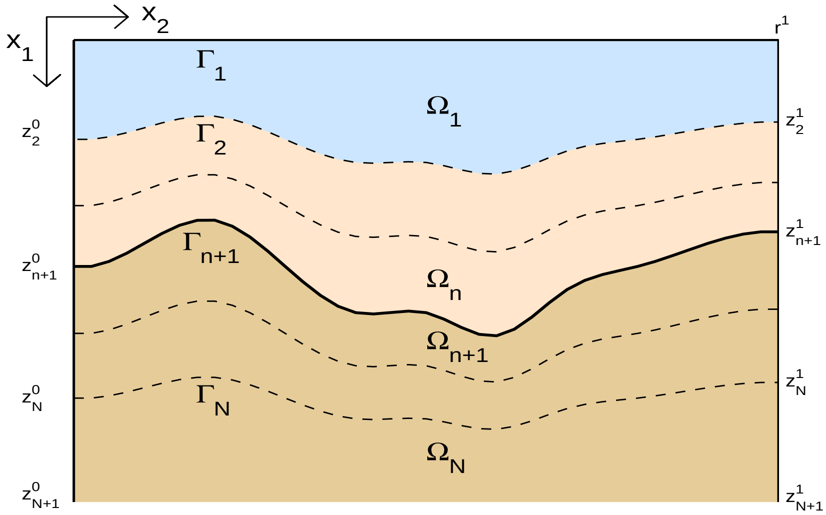

Figure 1: The physical domain.

equation, so within each layer

$$-\nabla \cdot \left(\frac{1}{\varrho}\nabla p\right) - \frac{\kappa^2}{\varrho} p = 0, \tag{1}$$

where $p(\boldsymbol{r})$ is the phasor of the acoustic pressure $\mathrm{Re}\big(p(\boldsymbol{r})\exp(-i2\pi f t)\big)$ [2, p. 5]. The density ϱ of the layered medium is constant within each layer. The wavenumber κ is given by $\kappa = \frac{2\pi f}{c}(1 + i\delta)$, where the sound speed c and the loss tangent δ may depend on the space coordinates in the top n layers but are constant in the homogeneous layers. The attenuation $\mathrm{Im}(\kappa)$ is *required* to be nonzero only in the bottom layer Ω_N.

The problem is originally three-dimensional but in order to make it computationally tractable, we use either a plane-symmetric or an axisymmetric two-dimensional restriction of the problem.

2.1 Differential formulation

The plane-symmetric or axisymmetric two-dimensional restriction of equation (1) for the layer Ω_d is given by

$$-\frac{\partial}{\partial x_1}\Big(\frac{1}{\varrho_d}\frac{\partial p_d}{\partial x_1}\Big) - \frac{1}{\eta}\frac{\partial}{\partial x_2}\Big(\frac{\eta}{\varrho_d}\frac{\partial p_d}{\partial x_2}\Big) - \frac{\kappa_d^2}{\varrho_d} p_d = 0, \tag{2}$$

where p_d is the pressure, ϱ_d is the density, and κ_d is the wavenumber in the domain Ω_d, $d = 1, \ldots, N$. Plane symmetry means that the coordinates (x_1, x_2) are translated into the Cartesian coordinates (x, y, z) as $z = x_1$, $x = x_2$, and that the pressure is independent of y. Axial symmetry means that the coordinates are related to cylindrical coordinates (r, ϕ, z) by $z = x_1$, $r = x_2 + r^0$, and that the pressure is independent of the azimuthal angle ϕ. The parameter r^0 is the radial distance from the sound source (located on the z-axis) to the near-field boundary ($x_2 = 0$). The scale factor η is given by $\eta = 1$ for plane symmetry and $\eta(x_2) = x_2 + r^0$ for the axisymmetric case.

2.2 Boundary integral formulation

Using Green's formula for equation (1), an integral representation of the solution $p(\boldsymbol{r}')$ can be derived at any field point $\boldsymbol{r}'$ in the homogeneous domain Ω_d resulting in

$$p_d(\boldsymbol{r}') = \int\limits_{S_d} \Big(G_d(\boldsymbol{r}', \boldsymbol{r}) \frac{\partial p_d}{\partial n}(\boldsymbol{r}) - \frac{\partial G_d}{\partial n}(\boldsymbol{r}', \boldsymbol{r}) p_d(\boldsymbol{r}) \Big)\, dS, \quad d = n+1, \ldots, N,$$

where $G_d(\boldsymbol{r}', \boldsymbol{r})$ is the free-space Green's function [14, p. 805], $\frac{\partial}{\partial n} = \boldsymbol{n} \cdot \nabla$, and $\boldsymbol{n}$ is the outward unit normal to the boundary S_d of Ω_d.

In the limit where $\boldsymbol{r}'$ tends to the boundary, a so-called boundary integral equation (BIE) can be derived [22, Sec. 2.5.4] for the solution at the boundary:

$$(3) \qquad \tfrac{1}{2} p_d(\boldsymbol{r}') + \int\limits_{S_d} \Big(\frac{\partial G_d}{\partial n}(\boldsymbol{r}', \boldsymbol{r}) p_d(\boldsymbol{r}) - G_d(\boldsymbol{r}', \boldsymbol{r}) \frac{\partial p_d}{\partial n}(\boldsymbol{r}) \Big)\, dS = 0, \quad \boldsymbol{r}' \in S_d.$$

Thus, the solution inside Ω_d could be computed once the solution has been determined on the boundary S_d.

In the case of plane symmetry, the two-dimensional Green's function $G_d(\boldsymbol{x}', \boldsymbol{x})$ is equal to $\frac{i}{4} \mathrm{H}_0^{(1)}(\kappa_d |\boldsymbol{x}' - \boldsymbol{x}|)$ for outgoing waves [22, p. 177] and $-\frac{i}{4} \mathrm{H}_0^{(2)}(\kappa_d |\boldsymbol{x}' - \boldsymbol{x}|)$ for incoming waves, where $\mathrm{H}_0^{(1)}$ and $\mathrm{H}_0^{(2)}$ are the zeroth order Hankel functions [14, p. 623] of the first and second kinds, respectively. For axial symmetry, the restricted Green's function is $G_d(\boldsymbol{x}', \boldsymbol{x}) = \int_0^{2\pi} \frac{\exp(\pm i\kappa_d |\boldsymbol{r}' - \boldsymbol{r}|)}{4\pi |\boldsymbol{r}' - \boldsymbol{r}|}\, d\phi$ for outgoing and incoming waves, respectively. Since there are no sinks present, outgoing waves only are admissible. Thus, the Green's function is

$$G_d(\boldsymbol{x}', \boldsymbol{x}) = \frac{i}{4} \mathrm{H}_0^{(1)}(\kappa_d |\boldsymbol{x}' - \boldsymbol{x}|) \quad \text{or} \quad G_d(\boldsymbol{x}', \boldsymbol{x}) = \frac{1}{4\pi} \int\limits_0^{2\pi} \frac{\exp(i\kappa_d |\boldsymbol{r}' - \boldsymbol{r}|)}{|\boldsymbol{r}' - \boldsymbol{r}|}\, d\phi,$$

and its normal derivative is given by

$$\frac{\partial G_d}{\partial n}(\boldsymbol{x}', \boldsymbol{x}) = \boldsymbol{n} \cdot \nabla G_d = \frac{i\kappa_d}{4} \mathrm{H}_1^{(1)}(\kappa_d |\boldsymbol{x}' - \boldsymbol{x}|) \frac{(\boldsymbol{x}' - \boldsymbol{x}) \cdot \boldsymbol{n}}{|\boldsymbol{x}' - \boldsymbol{x}|}$$

or

$$\frac{\partial G_d}{\partial n}(\boldsymbol{x}', \boldsymbol{x}) = \frac{1}{4\pi} \int\limits_0^{2\pi} (|\boldsymbol{r}' - \boldsymbol{r}|^{-1} - i\kappa_d) \exp(i\kappa_d |\boldsymbol{r}' - \boldsymbol{r}|) \frac{(\boldsymbol{r}' - \boldsymbol{r}) \cdot \boldsymbol{n}}{|\boldsymbol{r}' - \boldsymbol{r}|^2}\, d\phi.$$

2.3 Boundary and interface conditions

In addition to equation (2) or (3), boundary and interface conditions are needed (in order to couple the solutions between neighboring domains).

On the surface boundary Γ_1, pressure release is imposed:

$$p_1(0, x_2) = 0. \tag{4}$$

On the interfaces between fluid layers, the pressure and the normal velocity are required to be continuous, i.e.,

$$p_d(\boldsymbol{x}) = p_{d+1}(\boldsymbol{x}), \tag{5a}$$

$$\frac{1}{\varrho_d}\frac{\partial p_d}{\partial n}(\boldsymbol{x}) = \frac{1}{\varrho_{d+1}}\frac{\partial p_{d+1}}{\partial n}(\boldsymbol{x}), \quad \boldsymbol{x} \in \Gamma_{d+1}, \quad d = 1, \ldots, N-1, \tag{5b}$$

where $\boldsymbol{n}$ is a unit normal at the interface Γ_{d+1} between Ω_d and Ω_{d+1}.

For computational reasons, we truncate the depth of the last layer. When its attenuation and thickness are large enough, the pressure becomes close to zero at the bottom. Hence, we choose an appropriately matching thickness and use the boundary conditions

$$p_N \to 0 \quad \text{as } x_1 \to \infty, \text{ and consequently} \tag{6a}$$

$$\nabla p_N \to 0 \quad \text{as } x_1 \to \infty, \tag{6b}$$

in order to neglect p_N and $\frac{\partial p_N}{\partial n}$ for $\boldsymbol{x}$ along the artificial bottom Γ_{N+1}.

It is somewhat awkward to determine an appropriate layer thickness a priori, since the vertical attenuation of the solution is known typically only a posteriori. Furthermore, it is desirable to avoid costly discretizations of potentially thick layers. In future work, we intend to develop a truncation technique based on sharper a priori attenuation estimates. During the initial development of the BIE method, it would be reasonable to simplify the problem by treating Γ_N as a rigid boundary ($\frac{\partial p_N}{\partial n} = 0$ along Γ_N) and omitting Ω_N.

3 Radiation boundary conditions

For computational reasons, the range of the domain has to be truncated. This is done by introducing a far-field boundary at $x_2 = r^1$ and a near-field boundary at $x_2 = 0$. These artificial boundaries should be transparent to all waves. We emulate this by employing nonlocal Dirichlet-to-Neumann (DtN) maps [9].

3.1 Normal modes

Boundary conditions based on DtN maps require the boundary in question to be a separable coordinate surface. Our design of radiation boundary conditions follows the principles in [6, 17, 12]. Thus, it is assumed that the bathymetry *beyond* each artificial boundary is horizontally stratified. Under this assumption and the separability requirement that κ depends only on the depth x_1 (in the two horizontally stratified regions), the Helmholtz equations (2) can be solved by separation of variables. The ansatz $p(x_1, x_2) = \psi(x_1)\chi(x_2)$ leads to

$$-\chi\varrho(x_1)\frac{d}{dx_1}\Big(\frac{1}{\varrho(x_1)}\frac{d\psi}{dx_1}\Big) - \frac{\psi}{\eta(x_2)}\frac{d}{dx_2}\Big(\eta(x_2)\frac{d\chi}{dx_2}\Big) - \kappa^2(x_1)\psi\chi = 0.$$

The separation ansatz $\frac{1}{\eta\chi}\frac{d}{dx_2}\big(\eta\frac{d\chi}{dx_2}\big) = \lambda$ yields the following eigenproblem:

$$-\frac{d}{dx_1}\Big(\frac{1}{\varrho}\frac{d\psi}{dx_1}\Big) - \frac{\kappa^2}{\varrho}\psi = \frac{\lambda}{\varrho}\psi$$

with boundary conditions (4), (5), and (6a) taking the form

$$\begin{aligned} &\psi(0) = 0, \\ &\psi \text{ and } \tfrac{1}{\varrho}\tfrac{d\psi}{dx_1} \text{ are continuous at } x_1 = z_d,\ d = 2, \dots, N, \\ &\psi(z_{N+1}) = 0, \end{aligned}$$

where N is the number of fluid layers. This Sturm–Liouville problem can be solved numerically by, e.g., FEM [15, 12] to find an approximant $\widetilde{\psi}_m(x_1)$ to $\psi_m(x_1)$ and an approximation of λ_m for the mth eigenpair.

For $\lambda_m \neq 0$, the ordinary differential equation for the propagator $\chi(x_2)$ yields exponential functions

$$\chi_m(x_2) = A_m \exp(i\sqrt{-\lambda_m}x_2) + B_m \exp(-i\sqrt{-\lambda_m}x_2), \quad m = 1, 2, \dots$$

in the case of plane symmetry, and Hankel functions

$$\chi_m(x_2) = A_m \frac{\mathrm{H}_0^{(1)}(\sqrt{-\lambda_m}(x_2 + r^0))}{\mathrm{H}_0^{(1)}(\sqrt{-\lambda_m}r^0)} + B_m \frac{\mathrm{H}_0^{(2)}(\sqrt{-\lambda_m}(x_2 + r^0))}{\mathrm{H}_0^{(2)}(\sqrt{-\lambda_m}r^0)}, \quad m = 1, 2, \dots$$

for axial symmetry. The functions are scaled to get $\chi_m(0) = A_m + B_m$ for both plane and axial symmetry.

The separated solution $p(x_1, x_2)$ is a mode sum of $\psi_m(x_1)\chi_m(x_2)$ over all possible m. For practical reasons the sum must be truncated in an appropriate way. We devise a truncation based on loss angles [8, p. 134]. Assume that the eigenvalues λ_m are sorted in descending order after $\mathrm{Re}(\sqrt{-\lambda_m})$, and let θ denote the largest allowed loss angle. Modes are included if they satisfy the following attenuation criterion

$$\mathrm{Im}(\sqrt{-\lambda_m}) \leq \min\big(\tan(\theta)\mathrm{Re}(\sqrt{-\lambda_m}), \alpha\big),$$

where α is an optional tolerance. The cut-off index μ is the highest index for which the attenuation criterion holds. It is different for the near-field (μ_0) and far-field (μ_1) boundaries.

3.2 DtN conditions

The eigenfunctions ψ_m are conjugate with respect to the bilinear form

$$\langle f, g\rangle \equiv \int_0^{z_{N+1}} \frac{1}{\varrho} f(z) g(z) dz,$$

which means that $\langle \psi_m, \psi_n\rangle = \delta_{mn}$. This property is used for expressing the coefficients B_m. At the near-field boundary ($x_2 = 0$), the coefficients A_m characterize the source term so we consider them as known. If we take the bilinear form of the separated solution (expressed as a truncated mode sum) and an eigenfunction ψ^0_m, then because of the conjugacy of the eigenfunctions, we get an expression for the coefficients

$$B_m = \langle \psi^0_m, p(\cdot, 0)\rangle - A_m.$$

After differentiating the truncated mode sum with respect to x_2 and eliminating B_m, we obtain the boundary condition

$$(7)\quad -\frac{\partial p}{\partial x_2}(x_1, 0) + \sum_{m=1}^{\mu_0} C^0_m \langle \psi^0_m, p(\cdot, 0)\rangle \psi^0_m(x_1) = \sum_{m=1}^{\mu_0} A^0_m \psi^0_m(x_1), \quad 0 \le x_1 \le z^0_{N+1},$$

where

$$C^0_m = \begin{cases} -i\sqrt{-\lambda^0_m} & \text{for plane symmetry,} \\ -\sqrt{-\lambda^0_m}\,\frac{\mathrm{H}^{(2)}_1}{\mathrm{H}^{(2)}_0}\big(\sqrt{-\lambda^0_m} r^0\big) & \text{for axial symmetry,} \end{cases}$$

$$A^0_m = \begin{cases} -2i\sqrt{-\lambda^0_m} A_m & \text{for plane symmetry,} \\ A_m \sqrt{-\lambda^0_m}\Big(\frac{\mathrm{H}^{(1)}_1}{\mathrm{H}^{(1)}_0}\big(\sqrt{-\lambda^0_m} r^0\big) - \frac{\mathrm{H}^{(2)}_1}{\mathrm{H}^{(2)}_0}\big(\sqrt{-\lambda^0_m} r^0\big)\Big) & \text{for axial symmetry.} \end{cases}$$

The boundary condition at the far-field boundary ($x_2 = r^1$) is derived in a similar way. The coefficients $B_m = 0$ because there are only outgoing waves, the coefficients A_m are calculated as $A_m = \langle \psi^1_m, p(\cdot, r^1)\rangle$, and the condition becomes

$$(8)\qquad \frac{\partial p}{\partial x_2}(x_1, r^1) + \sum_{m=1}^{\mu_1} C^1_m \langle \psi^1_m, p(\cdot, r^1)\rangle \psi^1_m(x_1) = 0, \quad 0 \le x_1 \le z^1_{N+1},$$

where

$$C^1_m = \begin{cases} -i\sqrt{-\lambda^1_m} & \text{for plane symmetry,} \\ \sqrt{-\lambda^1_m}\,\frac{\mathrm{H}^{(1)}_1}{\mathrm{H}^{(1)}_0}\big(\sqrt{-\lambda^1_m}(r^1 + r^0)\big) & \text{for axial symmetry.} \end{cases}$$

For a standing wave mode, which corresponds to $\lambda_\mu^0 = 0$ (or $\lambda_\mu^1 = 0$), the coefficients C_μ^0 and A_μ^0 in (7) would not determine a unique solution. For $\lambda_\mu^0 = 0$, an appropriate choice is

$$C_\mu^0 = \begin{cases} 1 & \text{for plane symmetry,} \\ \dfrac{1}{r^0 \ln(r^0)} & \text{for axial symmetry,} \end{cases}$$

$$A_\mu^0 = \begin{cases} A_\mu & \text{for plane symmetry,} \\ \dfrac{A_\mu}{r^0 \ln(r^0)} & \text{for axial symmetry,} \end{cases}$$

whereas $C_\mu^1 = 0$ is adequate for $\lambda_\mu^1 = 0$.

A similar uniqueness issue is well known from the literature on boundary element methods for scattering problems. For exterior problems, a straightforward use of a BIE like (3) may fail for isolated wavenumbers [20], due to nonphysical singularities associated with eigenmodes of a related problem for the interior domain. BIE formulations without such artificial singularities could be obtained by a linear combination of an equation like (3) and its counterpart for the normal derivative [3]. In order to investigate whether this phenomenon occurs for any waveguide problems under consideration, a study of the smallest singular value of the resulting coefficient matrix, as a function of wavenumber, is warranted. Such an investigation is also motivated to assess the sensitivity of the DtN conditions for cases where wavenumber variations cause λ_μ^0 or λ_μ^1 to approach zero.

4 Specification of the differential formulation

4.1 Boundary fitted coordinates

For the top n layers, we use the finite difference method constructed in [15, 12]. In this context, it is convenient to use boundary conforming coordinates [10, p. 5]. We introduce the logical coordinates ξ_1 and ξ_2, and perform orthogonal transformations from squares ($d-1 \le \xi_1 \le d, 0 \le \xi_2 \le 1$) onto the domains $(x_1(\xi_1,\xi_2), x_2(\xi_1,\xi_2)) \in \Omega_d$ for $d = 1,\ldots,n$. Under such transformations, the Helmholtz equation (2) becomes

$$-\frac{\partial}{\partial \xi_1}\Big(\frac{\eta}{\varrho_d}\frac{\eta_{2,d}}{\eta_{1,d}}\frac{\partial p_d}{\partial \xi_1}\Big) - \frac{\partial}{\partial \xi_2}\Big(\frac{\eta}{\varrho_d}\frac{\eta_{1,d}}{\eta_{2,d}}\frac{\partial p_d}{\partial \xi_2}\Big) - \eta\,\eta_{1,d}\eta_{2,d}\frac{\kappa_d^2}{\varrho_d}p_d = 0, \tag{9}$$

where $\eta_{1,d}$ and $\eta_{2,d}$ are the scale factors. The corresponding interface conditions (5) are transformed into

$$p_d(d,\xi_2) = p_{d+1}(d,\xi_2), \tag{10}$$

$$\frac{1}{\varrho_d \eta_{1,d}}\frac{\partial p_d}{\partial \xi_1}(d,\xi_2) = \frac{1}{\varrho_{d+1}\eta_{1,d+1}}\frac{\partial p_{d+1}}{\partial \xi_1}(d,\xi_2), \tag{11}$$

for $0 \leq \xi_2 \leq 1$, $d = 1, \ldots, n-1$. For the discretization method in [12], the conditions (10) and (4) are inherently satisfied through the choices of the grid and the degrees of freedom.

4.2 Linearized coordinate transformations

We do not transform Ω_d, $d = n+1, \ldots, N$, since it is considerably more convenient to solve the BIE (3) in the coordinates (x_1, x_2). Furthermore, the DtN conditions (7) and (8) are stated in these coordinates even for the transformed domains. Hence, the normal derivative $\frac{\partial p}{\partial n}$ (at the vertical boundaries) needs to be transformed from logical space to $\boldsymbol{x}$-space for the top n layers. In the vicinity of the vertical boundaries, the interfaces are assumed to be horizontal. Consequently, the coordinate transformation is approximated well by linearization. Close to the near-field boundary, we employ the following linearization

$$(12) \quad \begin{cases} x_1 = z_d^0 + (\xi_1 - (d-1))(z_{d+1}^0 - z_d^0), & d-1 \leq \xi_1 \leq d, \quad d = 1, \ldots, n, \\ x_2 = \xi_2 \eta_{2,d}(d-1, 0), & \xi_2 \approx 0. \end{cases}$$

At the far-field boundary, we use

$$(13) \quad \begin{cases} x_1 = z_d^1 + (\xi_1 - (d-1))(z_{d+1}^1 - z_d^1), & d-1 \leq \xi_1 \leq d, \quad d = 1, \ldots, n, \\ x_2 = r^1 + (\xi_2 - 1)\eta_{2,d}(d-1, 1), & \xi_2 \approx 1. \end{cases}$$

Under this local coordinate transformation, the normal derivative $\frac{\partial p}{\partial x_2}$ can easily be obtained from $\frac{\partial p}{\partial \xi_2}$.

5 Specification of the boundary integral formulation

For the homogeneous domains, we use the BIE (3) formulation of the Helmholtz equation in a two-dimensional (restricted) case. Consequently, the corresponding two-dimensional Green's function is used and the field point $\boldsymbol{r}'$ is replaced by $\boldsymbol{x}'$. The boundary element dS is either $\eta d\gamma$ (plane symmetry) or $\eta d\phi d\gamma$ (axial symmetry), where η is the scale factor in (2) and $d\gamma$ is the arc length element of either the *curve* S_d or the envelope generating the rotational *surface* S_d. The integral equations in Section 2.2 are stated domainwise, but are now split into contributions from subboundaries in order to facilitate the incorporation of the interface conditions. For each domain Ω_d, $d = n+1, \ldots, N$, the integral in (3) can be written as a sum of four subintegrals

$$\int_{S_d} = \int_{z_d^0}^{z_{d+1}^0} + \int_{\Gamma_d} + \int_{z_d^1}^{z_{d+1}^1} + \int_{\Gamma_{d+1}} \equiv I_{d,0} + I_{d,\frac{1}{2}} + I_{d,1} + I_{d,\frac{3}{2}},$$

where the entire boundary

$$S_d = \begin{cases} [z_d^0, z_{d+1}^0] \cup \Gamma_d \cup [z_d^1, z_{d+1}^1] \cup \Gamma_{d+1} & \text{for plane symmetry,} \\ \{[z_d^0, z_{d+1}^0] \cup \Gamma_d \cup [z_d^1, z_{d+1}^1] \cup \Gamma_{d+1}\} \times [0, 2\pi] & \text{for axial symmetry.} \end{cases}$$

All the integrals $I_{d,\beta}$ are one-dimensional, even for the axisymmetric case. For axial symmetry, the integration in (3) over the azimuthal coordinate ϕ is done separately *only* for $G_d(\boldsymbol{r}', \boldsymbol{r})$ and $\frac{\partial G_d}{\partial n}(\boldsymbol{r}', \boldsymbol{r})$, since the solution is independent of ϕ. That yields the restricted Green's function in Section 2.2 and leaves one-dimensional integrals with integration element $\eta d\gamma$ also for axial symmetry.

At each interface Γ_{d+1}, $d = n+1, \ldots, N-1$, there are originally four unknowns p_{d+1}, $\frac{\partial p_{d+1}}{\partial n}$, p_d, $\frac{\partial p_d}{\partial n}$ appearing in the boundary integral equations for S_{d+1} and S_d as well as in the two interface conditions (5). Due to the simple structure of the interface conditions, we find it suitable to use them to eliminate p_d and $\frac{\partial p_d}{\partial n}$ along the bottom interface Γ_{d+1} of Ω_d. Thus, there will remain two unknowns appearing in two BIEs for each interface. At each vertical boundary of Ω_d, $d = n+1, \ldots, N$, there are two unknowns appearing in the BIE for S_d and in the DtN condition (7) or (8).

5.1 The interface condition along the hybrid interface

At the hybrid (between PDE and BIE) interface Γ_{n+1}, we choose a representation of the solution that is appropriate for the BIE formulation (3) used for the domain Ω_{n+1}. That representation of the pressure is $p_{n+1}\big(x_1(n, \xi_2), x_2(n, \xi_2)\big)$, by which $p_n\big(x_1(n, \xi_2), x_2(n, \xi_2)\big)$ is replaced in order to enforce condition (5a) for $d = n$. The formulations (5b) and (11) of the remaining interface condition are combined to yield

$$(14) \qquad -\frac{1}{\varrho_n \eta_{1,n}} \frac{\partial p_n}{\partial \xi_1}(d, \xi_2) = \frac{1}{\varrho_{n+1}} \frac{\partial p_{n+1}}{\partial n}(x_1(d, \xi_2), x_2(d, \xi_2)), \quad d = n,$$

where $\boldsymbol{n}$ is the unit normal vector pointing out of the domain Ω_{n+1}.

5.2 Integrals along the top interfaces

Along the top interface Γ_d of Ω_d, $d = n+1, \ldots, N$, we obtain

$$(15) \qquad I_{d,\frac{1}{2}}(\boldsymbol{x}') = \int_{\Gamma_d} \Big(\frac{\partial G_d}{\partial n} p_d(\boldsymbol{x}) - G_d \frac{\partial p_d}{\partial n}(\boldsymbol{x}) \Big) \eta \, d\gamma.$$

5.3 Integrals along the bottom interfaces

For the integral along the bottom interface Γ_{d+1}, $d = n+1, \dots, N-1$, appearing in the BIE for S_d, we eliminate p_d and $\frac{\partial p_d}{\partial n}$ by exploiting the interface conditions (5). So the integral along the bottom interface of Ω_d becomes

$$I_{d,\frac{3}{2}}(\boldsymbol{x}') = \int\limits_{\Gamma_{d+1}} \Big(\frac{\partial G_d}{\partial n} p_{d+1}(\boldsymbol{x}) - G_d \frac{\varrho_d}{\varrho_{d+1}} \frac{\partial p_{d+1}}{\partial n}(\boldsymbol{x})\Big) \eta \, d\gamma. \tag{16a}$$

Along the artificial bottom Γ_{N+1}, the integrand from (15) would be appropriate for $d = N$. However, based on conditions (6) and the explanation in Section 2.3, we impose the approximation

$$I_{N,\frac{3}{2}} \approx 0. \tag{16b}$$

5.4 Integrals along the vertical boundaries

Since the vertical boundaries are coordinate curves, they are readily parametrized by the coordinate x_1 implying that the arc length element $d\gamma = dx_1$. The normal derivative $\frac{\partial}{\partial n} \equiv \boldsymbol{n} \cdot \nabla$ becomes $-\frac{\partial}{\partial x_2}$ at the near-field boundary ($x_2 = 0$) and $\frac{\partial}{\partial x_2}$ at the far-field boundary ($x_2 = r^1$). Along the vertical boundaries of domain Ω_d, $d = n+1, \dots, N$, we get the integrals

$$I_{d,0}(\boldsymbol{x}') = \eta(0) \int\limits_{z_d^0}^{z_{d+1}^0} \Big(-\frac{\partial G_d}{\partial x_2} p_d(x_1, 0) - G_d \frac{\partial p_d}{\partial n}(x_1, 0)\Big) dx_1, \tag{17}$$

$$I_{d,1}(\boldsymbol{x}') = \eta(r^1) \int\limits_{z_d^1}^{z_{d+1}^1} \Big(\frac{\partial G_d}{\partial x_2} p_d(x_1, r^1) - G_d \frac{\partial p_d}{\partial n}(x_1, r^1)\Big) dx_1. \tag{18}$$

5.5 Boundary integral equations

We now state the boundary integral equations involving the integrals $I_{d,\beta}(\boldsymbol{x}')$ given by (15–18). For field points at the vertical boundaries of the domain Ω_d, $d = n+1, \dots, N$, the equations become

$$\tfrac{1}{2} p_d(x_1', 0) + I_{d,0} + I_{d,\frac{1}{2}} + I_{d,1} + I_{d,\frac{3}{2}} = 0, \quad x_1' \in [z_d^0, z_{d+1}^0], \tag{19}$$

$$\tfrac{1}{2} p_d(x_1', r^1) + I_{d,0} + I_{d,\frac{1}{2}} + I_{d,1} + I_{d,\frac{3}{2}} = 0, \quad x_1' \in [z_d^1, z_{d+1}^1]. \tag{20}$$

Placing the field point $\boldsymbol{x}'$ at the top interface of Ω_d yields

$$\tfrac{1}{2} p_d(\boldsymbol{x}') + I_{d,0} + I_{d,\frac{1}{2}} + I_{d,1} + I_{d,\frac{3}{2}} = 0, \quad \boldsymbol{x}' \in \Gamma_d, \quad d = n+1, \dots, N. \tag{21}$$

At the bottom interface of Ω_{d-1}, we obtain

$$(22)\quad \tfrac{1}{2}p_d(\boldsymbol{x}') + I_{d-1,0} + I_{d-1,\frac{1}{2}} + I_{d-1,1} + I_{d-1,\frac{3}{2}} = 0, \quad \boldsymbol{x}' \in \Gamma_d, \quad d = n+2,\dots,N.$$

According to the previously described elimination strategy, the interface condition (5a) has been employed to substitute p_d for p_{d-1} in (22).

6 Discretization

In the previous sections, we have specified the partial differential equations and the boundary integral equations that are subject to hybridization. The complete hybrid model consists of the PDE (9) and the interface condition (11) for the top n layers, the interface condition (14) for the hybrid interface, the BIEs (19–22) for the boundaries of the remaining layers, and the DtN conditions (7) and (8) for the vertical boundaries. The remaining sections concern mainly the discretization of the BIEs and the DtN conditions. For details about the finite difference method used for (9) and (11), we refer to [15, 12, 17].

6.1 Parametrization of interfaces

For the numerical treatment of the integrals (15–16a), it is necessary to parametrize each interface Γ_d, $d = n+1,\dots,N$. Let the parameter $t \in [0,1]$ be the abscissa to the locus $(x_1(t), x_2(t)) \in \Gamma_d$, where $x_2(t)$ is an increasing function. The scale factor for such a parametrization is $\eta_{t,d} = \sqrt{\left(\frac{dx_1}{dt}\right)^2 + \left(\frac{dx_2}{dt}\right)^2}$ and the arc length element is given by $d\gamma = \eta_{t,d}\, dt$. For either plane or axial symmetry, the outward pointing normal vectors on Γ_d become

$$\boldsymbol{n} = \begin{cases} \frac{1}{\eta_{t,d}}\frac{dx_2}{dt}\widehat{\boldsymbol{x}}_1 - \frac{1}{\eta_{t,d}}\frac{dx_1}{dt}\widehat{\boldsymbol{x}}_2 & \text{for } \Omega_{d-1}, \\ -\frac{1}{\eta_{t,d}}\frac{dx_2}{dt}\widehat{\boldsymbol{x}}_1 + \frac{1}{\eta_{t,d}}\frac{dx_1}{dt}\widehat{\boldsymbol{x}}_2 & \text{for } \Omega_d, \end{cases}$$

and the normal derivative is $\frac{\partial}{\partial n} \equiv \boldsymbol{n}\cdot\nabla = n_1\frac{\partial}{\partial x_1} + n_2\frac{\partial}{\partial x_2}$.

Due to the interface condition (14), it is convenient to parametrize the hybrid interface Γ_{n+1} by the logical coordinate $\xi_2 \in [0,1]$ defined in Section 4.1, which yields $d\gamma = \eta_{2,n}(n,\xi_2)d\xi_2$.

6.2 Grids

In order to discretize the boundary integral equations for each interface Γ_d, $d = n+1,\dots,N$, we introduce (typically nonequidistant) node points

$$0 = t^0 < t^1 < \cdots < t^{m_{\frac{1}{2},d}} = 1$$

for the coordinate $t \in [0,1]$ parametrizing Γ_d. The corresponding element lengths are given by

$$h_d^j = t^j - t^{j-1}, \quad j = 1, \dots, m_{\frac{1}{2},d}.$$

For the logical coordinate ξ_2 parametrizing the interfaces Γ_d, $d = 2, \dots, n$, the following equidistant grid is used

$$\xi_2^j = \left(j - \tfrac{3}{2}\right) h_2, \quad j = 1, \dots, m_2,$$

where $h_2 = \frac{1}{m_2 - 2}$.

For each portion $x_1 \in [z_d^b, z_{d+1}^b]$, $d = n+1, \dots, N$, $b = 0, 1$, of the vertical boundaries, we use a uniform grid

$$x_1^j = z_d^b + j h_{b,d}, \quad j = 0, \dots, m_{b,d},$$

where $h_{b,d} = \frac{z_{d+1}^b - z_d^b}{m_{b,d}}$. The discretization technique could easily be modified to accommodate nonuniform grids also for the x_1-coordinate, but there is no apparent reason for those. In the discretization of the DtN conditions for the first n domains, it is convenient to slightly modify the enumeration of the node points. So for $x_1 \in [z_d^b, z_{d+1}^b]$, $d = 1, \dots, n$, $b = 0, 1$, the grid is chosen as

$$x_1^j = z_d^b + j h_{b,d}, \quad j = 0, \dots, m_{1,d} + 1,$$

where $h_{b,d} = \frac{z_{d+1}^b - z_d^b}{m_{1,d}+1}$. Note that the coordinate transformations (12) and (13) applied to the uniform distribution of node points ξ_1^j, $j = 0, \dots, m_{1,d} + 1$, (compatible with [12]) for $\xi_1 \in [\, d-1, d\,]$ yield the grids above.

The differential formulation of the Helmholtz equation given in Section 4.1 and the Sturm–Liouville problem for the normal modes in Section 3.1 are both discretized by fourth-order accurate methods. For convenience and compatibility reasons, we choose to discretize the boundary integral equations by employing the same type of basis functions as for the FEM for the Sturm–Liouville problem.

6.3 Approximants to the pressure and its normal derivative

Consider a given set of node points $\{t^j\}_{j=0}^{m_{\frac{1}{2},d}}$. The basis functions mentioned above are piecewise linear functions $\widehat{\varphi}_{j,1}(t)$ with support on $[t^{j-1}, t^{j+1}]$, and integrated piecewise Legendre polynomials $\widehat{\varphi}_{j,2}(t)$, $\widehat{\varphi}_{j,3}(t)$, which have support only for $t \in [t^{j-1}, t^j]$, i.e., element j. The four basis functions that have support on element j are defined by

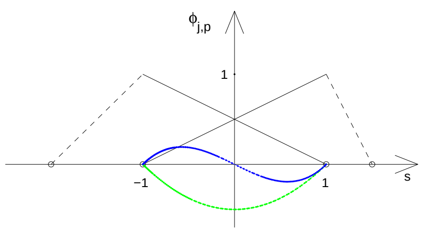

$$\begin{aligned}
\varphi_{j,1} &= \widehat{\varphi}_{j-1,1} = \tfrac{1}{2}(1-s) \\
\varphi_{j,2} &= \widehat{\varphi}_{j,2} = \tfrac{1}{2}(s^2-1) \\
\varphi_{j,3} &= \widehat{\varphi}_{j,3} = \tfrac{1}{2}(s^3-s) \\
\varphi_{j,4} &= \widehat{\varphi}_{j,1} = \tfrac{1}{2}(1+s)
\end{aligned}$$

where $s = \frac{2(t-t^j)}{h_d^j} + 1$, $t^{j-1} \leq t \leq t^j$, $j = 1, \ldots, m_{\frac{1}{2},d}$.

We let the approximants to the functions p and $\frac{\partial p}{\partial n}$ be denoted by ${}^{d,b}p^0$ and ${}^{d,b}p^1$. Index d refers to domain Ω_d, whereas b labels (for each Ω_d) the near-field boundary ($b = 0$), the top interface ($b = \frac{1}{2}$), and the far-field boundary ($b = 1$). We utilize a tensor notation [16, 1] obeying the Einstein summation convention, i.e., whenever an index is repeated both as subscript and superscript, a summation over the index is understood. An underlined index means that the summation convention is suppressed [18, p. 10] for that index. Hence, we can express each approximant as a linear combination of basis functions in the following way

$${}^{d,b}p^{\iota} = {}^{d,b}v^{\iota;0,1}\,\widehat{\varphi}_{0,1} + {}^{d,b}v^{\iota;j,p}\,\widehat{\varphi}_{j,p},$$

where ${}^{d,b}v^{\iota;j,p} \in \mathbb{C}$ are scalar coefficients.

Along the interfaces Γ_d, $d = n+1, \ldots, N$, we introduce the approximants

$$(23) \qquad {}^{d,\frac{1}{2}}p^{\iota}(t) = {}^{d,\frac{1}{2}}v^{\iota;0,1}\,\widehat{\varphi}_{0,1}(t) + {}^{d,\frac{1}{2}}v^{\iota;j,p}\,\widehat{\varphi}_{j,p}(t),$$

where $\iota = 0, 1$, $j = 1, \ldots, m_{\frac{1}{2},d}$, $p = 1, 2, 3$. Along the vertical boundaries, we obtain

$$(24) \qquad {}^{d,b}p^{\iota}(x_1) = {}^{d,b}v^{\iota;0,1}\,\widehat{\varphi}_{0,1}(x_1) + {}^{d,b}v^{\iota;j,p}\,\widehat{\varphi}_{j,p}(x_1)$$

for $x_1 \in [z_d^b, z_{d+1}^b]$, $d = n+1, \ldots, N$, $b = 0, 1$, $\iota = 0, 1$, $j = 1, \ldots, m_{b,d}$, $p = 1, 2, 3$.

For the top n layers, a finite difference technique based on node values is used. For notational uniformity, we label the node values with similar indices as for the coefficients of the approximants. Thus, we introduce

$${}^{d,\frac{1}{2}}v^{0;1,j} \approx p(d-1, \xi_2^j), \quad d = (1), 2, \ldots, n, \quad j = 1, \ldots, m_2$$

and

$${}^{d,1}v^{0;j,p} \approx p_d(\xi_1^j, \xi_2^p), \quad d = 1, \ldots, n, \quad j = 1, \ldots, m_{1,d}, \quad p = 1, \ldots, m_2.$$

Note that indices d and $\iota = 0$ have the same meaning as for the approximants used for the boundary integral equations. In this context, index $b = 1$ has a different meaning as well as indices j and p, which serve as node labels.

6.4 Compatibility conditions for the approximants

For the approximants, we enforce continuity of the pressure and its tangential derivatives at the node points $x_1 = z_d^b$, $b = 0, 1$, $d = n+1, \ldots, N$. For $x_1 = z_d^0$, $x_2 = 0$, the compatibility conditions become

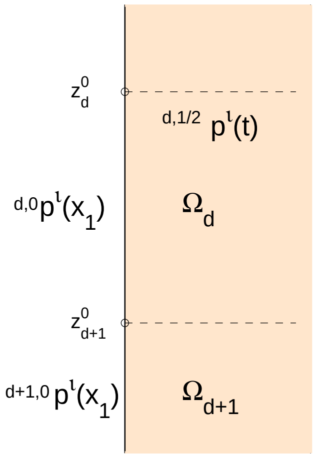

$$
\begin{aligned}
{}^{d,\frac{1}{2}}p^0(0) &= {}^{d,0}p^0(z_d^0),\\
{}^{d,\frac{1}{2}}p^1(0) &= -\frac{d}{dx_1}\left({}^{d,0}p^0\right)(z_d^0),\\
-\frac{d}{dt}\left({}^{d,\frac{1}{2}}p^0\right)(0) &= \eta_{t,d}(0)\,{}^{\underline{d},0}p^1(z_d^0), \quad d = n{+}1,\dots,N,\\
{}^{d,0}p^\iota(z_{d+1}^0) &= {}^{d+1,0}p^\iota(z_{d+1}^0), \quad d = n{+}1,\dots,N{-}1, \quad \iota = 0,1.
\end{aligned}
$$

In order to approximate the boundary condition (6a) consistently with the discretization of the boundary integrals and the normal modes, it is necessary to require that

$$
{}^{N,0}p^\iota(z_{N+1}^0) = 0, \quad \iota = 0,1.
$$

For $x_1 = z_d^1$, $x_2 = r^1$, analogous compatibility and consistency conditions arise.

By evaluating the approximants (with d replaced by δ), we can summarize the conditions as follows:

$$
\begin{aligned}
&(25) \qquad {}^{\delta,\beta}v^{\iota;m_{\beta,\delta},1} = {}^{\delta+1,\beta}v^{\iota;0,1}, \quad \beta = 0,1, \quad \iota = 0,1, \quad \delta = n+1,\dots,N-1,\\
&(26) \qquad {}^{N,\beta}v^{\iota;m_{\beta,N},1} = 0, \qquad \beta = 0,1, \quad \iota = 0,1,
\end{aligned}
$$

and

$$
\begin{aligned}
&(27a) \qquad {}^{\delta,\frac{1}{2}}v^{0;0,1} = {}^{\delta,0}v^{0;0,1},\\
&(27b) \qquad {}^{\delta,\frac{1}{2}}v^{0;j,1} = {}^{\delta,1}v^{0;0,1},
\end{aligned}
$$

$$
\begin{aligned}
&(28a) \qquad {}^{\delta,\frac{1}{2}}v^{1;0,1} = \frac{1}{h_{0,\delta}}\left({}^{\delta,0}v^{0;0,1} - {}^{\delta,0}v^{0;1,1} + 2\,{}^{\delta,0}v^{0;1,2} - 2\,{}^{\delta,0}v^{0;1,3}\right),\\
&(28b) \qquad {}^{\delta,\frac{1}{2}}v^{1;j,1} = \frac{1}{h_{1,\delta}}\left({}^{\delta,1}v^{0;0,1} - {}^{\delta,1}v^{0;1,1} + 2\,{}^{\delta,1}v^{0;1,2} - 2\,{}^{\delta,1}v^{0;1,3}\right),
\end{aligned}
$$

$$
\begin{aligned}
&(29a) \qquad {}^{\delta,\frac{1}{2}}v^{0;0,1} - {}^{\delta,\frac{1}{2}}v^{0;1,1} + 2\,{}^{\delta,\frac{1}{2}}v^{0;1,2} - 2\,{}^{\delta,\frac{1}{2}}v^{0;1,3} - h_\delta^1\eta_{t,\delta}(0)\,{}^{\underline{\delta},0}v^{1;0,1} = 0,\\
&(29b) \qquad -\,{}^{\delta,\frac{1}{2}}v^{0;j-1,1} + {}^{\delta,\frac{1}{2}}v^{0;j,1} + 2\,{}^{\delta,\frac{1}{2}}v^{0;j,2} + 2\,{}^{\delta,\frac{1}{2}}v^{0;j,3} - h_\delta^j\eta_{t,\delta}(1)\,{}^{\underline{\delta},1}v^{1;0,1} = 0,
\end{aligned}
$$

where $\delta = n+1,\dots,N$, $j = m_{\frac{1}{2},\delta}$.

We employ the conditions (25–28) to eliminate the coefficients on the left-hand sides from the ansatz of the corresponding approximants. The remaining unknown coefficients of the entire discretization method are

$$
\begin{array}{llll}
{}^{\delta,\frac{1}{2}}v^{0;1,p}, & \delta = 2,\dots,n, & p = 1,\dots,m_2, & \\
{}^{\delta,1}v^{0;j,p}, & \delta = 1,\dots,n, & j = 1,\dots,m_{1,\delta}, & p = 1,\dots,m_2, \\
{}^{\delta,\beta}v^{\iota;j,p}, & \delta = n+1,\dots,N, & \beta = 0,\tfrac{1}{2},1, \quad \iota = 0,1, & j = 1,\dots,m_{\beta,\delta}, \quad p = 1,2,3
\end{array}
$$

with the provisos that the combination $j = m_{\beta,\delta}$ and $p = 1$ is excluded, whereas $\beta = 0, 1$, $j = 0$, $p = 1$ is included.

6.5 Collocation

To determine the remaining coefficients for the approximants, it is necessary to state sufficiently many equations discretizing the boundary integral equations, the hybrid interface condition, and the DtN conditions. We choose to do this by a collocation method, whose guiding principles are

i) The boundary integral equations and the hybrid interface condition are collocated at two equidistant points inside every applicable element and at every applicable node point except at the artificial corners $x_1 = z_d^b$, $d = n+1,\dots,N+1$, $b = 0,1$.

ii) The DtN conditions are collocated at the two points inside every applicable element and at every applicable node point except $x_1 = z_{N+1}^b$, $b = 0,1$.

Thus, the collocation points for Γ_d are

$$
{}^{d}t^{k,q} = {}^{d}t^{k-1} + \tfrac{q-1}{3} h_d^k, \quad d = n+1,\dots,N, \quad k = 1,\dots,m_{\frac{1}{2},d}, \quad q = 1,2,3
$$

excluding ${}^{d}t^{1,1} = {}^{d}t^{0} = 0$. For the hybrid interface Γ_{n+1}, the node points are chosen such that

$$
{}^{n+1}t^{k-1} = \xi_2^k, \quad k = 2,\dots,m_{\frac{1}{2},n+1} = m_2 - 1.
$$

The collocation points for $x_1 \in [z_d^b, z_{d+1}^b]$ are

$$
{}^{d,b}x_1^{k,q} = {}^{d,b}x_1^{k-1} + \tfrac{q-1}{3} h_{b,d},\ d = n+1,\dots,N,\ b = 0,1,\ k = 1,\dots,m_{b,d},\ q = 1,2,3,
$$

where ${}^{d,b}x_1^{1,1} = z_d^b$ is excluded for the boundary integral equations.

The collocation points for the vertical boundaries $x_1 \in [z_d^b, z_{d+1}^b]$, $b = 0,1$, of the top n layers are

$$
\boldsymbol{x} = \begin{cases} (z_d^0, 0) \\ (z_d^1, r^1) \end{cases}, \quad d = 2,\dots,n,
$$

$$
\boldsymbol{x} = \begin{cases} ({}^{d,0}x_1^k, 0) \\ ({}^{d,1}x_1^k, r^1) \end{cases}, \quad d = 1,\dots,n, \quad k = 1,\dots,m_{1,d}.
$$

The compatibility conditions and the collocated equations constitute a system of equations that uniquely determines the coefficients ${}^{\delta,\beta}v^{\iota;j,p}$ listed above. In component form, the system of equations reads

$$ {}^{d,b}_{\delta,\beta}B^{e;k,q}_{\iota;j,p}\ {}^{\delta,\beta}v^{\iota;j,p} = {}^{d,b}g^{e;k,q}, $$

where B is the coefficient tensor and g is the right-hand side. The upper indices have partly different meanings than the lower ones. When the domain index ranges as $d = 1, \ldots, n$, the admissible ranges for the other upper indices are

$$ \begin{array}{llll} b = 1, & e = 1, & k = 1, \ldots, m_{1,d}, & q = 1, \ldots, m_2 \\ b = \frac{1}{2}, & e = 1, & k = 1, & q = 1, \ldots, m_2 \end{array} $$

Index b discriminates between internal ($b = 1$) collocation points and interface ($b = \frac{1}{2}$) points. The integers k and q are collocation node indices, and $e = 1$ is a (redundant) equation label.

For the domains where BIEs are used, the superscript ranges are

$$ d = n + 1, \ldots, N, \quad b = 0, \tfrac{1}{2}, 1, \quad e = 0, 1, \quad k = 1, \ldots, m_{b,d}, \quad q = 1, 2, 3, $$

where the combination $k = 1$ and $q = 1$ is excluded when $b = \frac{1}{2}$ or $b = 0, 1$ and $e = 0$. Index b is now a boundary label. The integers k and q are collocation element index and local collocation index, respectively. Combined with b, the label e serves as an identifier of equations subject to collocation. For the BIEs and DtN conditions, the labeling pattern is as follows. For $e = 0$, the boundary label $b = 0, \frac{1}{2}, 1$ refers to BIE (19), (21), (20), respectively. For $e = 1$, the values $b = 0, 1$ refer to DtN conditions (7) and (8), whereas $b = \frac{1}{2}$ identifies either BIE (22) or interface condition (14) for $d = n + 1$. The compatibility conditions (29) are labeled by exploiting the excluded values $k = 1$ and $q = 1$ for $e = 0$, $b = 0, 1$.

7 Assembly

The purpose of this section is to assemble the nonzero components of the coefficient tensor B and the right-hand side g. Those components of B that arise from the collocation of the boundary integral equations (19–21) are determined in two stages. Firstly, the approximants expressed as linear combinations of the basis functions $\widehat{\varphi}_{j,p}$ substitute p_d and $\frac{\partial p_d}{\partial n}$ in the integrals (15–18). The resulting integrals of linear combinations are rearranged into linear combinations of integrals. The latter integrals are partitioned elementwise in terms of the local basis functions $\varphi_{j,p}$, which makes it possible to efficiently exploit the local support of the basis functions. Secondly, the integral contributions to the components of B are assembled from the so-called element integrals listed in Appendix A. (This process is quite similar to the assembly of a global mass matrix from element mass matrices for a finite element method.)

7.1 Right-hand side

The nonzero components in the right-hand side all arise due to the source term in the DtN condition (7). For $b = 0, 1$, $m = 1, \ldots, \mu_b$, we define the following quantities pertaining to interfaces between the top n layers, nodes interior to the top n layers, and BIE collocation points

$$\begin{aligned}
{}^{d}_{b}\Psi_m &\equiv \widetilde{\psi}^b_m(z^b_d), && d = (1), 2, \ldots, n, \\
{}^{d}_{b}\Psi^k_m &\equiv \widetilde{\psi}^b_m({}^{d,b}x^k_1), && d = 1, \ldots, n, \quad k = 1, \ldots, m_{1,d}, \\
{}^{d}_{b}\Psi^{k,q}_m &\equiv \widetilde{\psi}^b_m({}^{d,b}x^{k,q}_1), && d = n+1, \ldots, N, \quad k = 1, \ldots, m_{b,d}, \quad q = 1, 2, 3,
\end{aligned}$$

where $\widetilde{\psi}^b_m$ is the finite element approximant to ψ^b_m. Using this notation, the nonzero components are given by

$$\begin{aligned}
{}^{d,\frac{1}{2}}g^{1;1,1} &= \sum_{m=1}^{\mu_0} A^0_m \, {}^{d}_{0}\Psi_m, && d = 2, \ldots, n, \\
{}^{d,1}g^{1;k,1} &= \sum_{m=1}^{\mu_0} A^0_m \, {}^{d}_{0}\Psi^k_m, && d = 1, \ldots, n, \quad k = 1, \ldots, m_{1,d}, \\
{}^{d,0}g^{1;k,q} &= \sum_{m=1}^{\mu_0} A^0_m \, {}^{d}_{0}\Psi^{k,q}_m, && d = n+1, \ldots, N, \quad k = 1, \ldots, m_{0,d}, \quad q = 1, 2, 3.
\end{aligned}$$

7.2 PDE and interface conditions

At interior points in the top n layers, the Helmholtz equation (9) is discretized by a nine-point Numerov scheme [15], causing the following tensor components to become nonzero

$$\begin{aligned}
&{}^{\underline{d},1}_{d,1}B^{1;k,q}_{0;j,p}, && d = 1, \ldots, n, && q = 2, \ldots, m_2 - 1, \quad p = q-1, q, q+1, \\
& && k = 1, \ldots, m_{1,d}, && j = k-1, k, k+1 \ \ (j \neq 0, m_{1,d}+1), \\
&{}^{\underline{d},1}_{d,\frac{1}{2}}B^{1;1,q}_{0;1,p}, && d = 2, \ldots, n, && q = 2, \ldots, m_2 - 1, \quad p = q-1, q, q+1, \\
&{}^{\underline{d},1}_{d+1,\frac{1}{2}}B^{1;m_{1,d},q}_{0;1,p}, && d = 1, \ldots, n-1, && q = 2, \ldots, m_2 - 1, \quad p = q-1, q, q+1, \\
&{}^{n,1}_{n+1,\frac{1}{2}}B^{1;m_{1,n},q}_{0;j,1}, && q = 2, \ldots, m_2 - 1, && j = q-2, q-1, q \ \ (j \neq 0, m_{\frac{1}{2},n+1}),
\end{aligned}$$

where the last components arise from the understanding that

$${}^{n,1}v^{0;m_{1,n}+1,j+1} \equiv {}^{n+1,\frac{1}{2}}v^{0;j,1}, \quad j = 1, \ldots, m_{\frac{1}{2},n+1} - 1$$

due to the following requirement of coinciding node points

$${}^{n+1}t^{j-1} = \xi^j_2, \quad j = 2, \ldots, m_{\frac{1}{2},n+1} = m_2 - 1.$$

Furthermore, extrapolation of the pressure approximant on the hybrid interface combined with elimination according to (27) yields

$$
\begin{aligned}
{}^{n,1}v^{0;m_{1,n}+1,1} &= 2\,{}^{n+1,0}v^{0;0,1} - {}^{n+1,\frac{1}{2}}v^{0;1,1} + 4\,{}^{n+1,\frac{1}{2}}v^{0;1,2} - 12\,{}^{n+1,\frac{1}{2}}v^{0;1,3},\\
{}^{n,1}v^{0;m_{1,n}+1,m_2} &= 2\,{}^{n+1,1}v^{0;0,1} - {}^{n+1,\frac{1}{2}}v^{0;j-1,1} + 4\,{}^{n+1,\frac{1}{2}}v^{0;j,2} + 12\,{}^{n+1,\frac{1}{2}}v^{0;j,3}, \quad j = m_{\frac{1}{2},n+1}
\end{aligned}
$$

resulting in the additional nonzero components

$$
\begin{aligned}
&{}^{n,1}_{n+1,0}B^{1;m_{1,n},2}_{0;0,1}, \qquad {}^{n,1}_{n+1,\frac{1}{2}}B^{1;m_{1,n},2}_{0;1,p}, \qquad p = 2,3,\\
&{}^{n,1}_{n+1,1}B^{1;m_{1,n},m_2-1}_{0;0,1}, \quad {}^{n,1}_{n+1,\frac{1}{2}}B^{1;m_{1,n},m_2-1}_{0;j,p}, \quad p = 2,3, \quad j = m_{\frac{1}{2},n+1}.
\end{aligned}
$$

The interface conditions (11) are discretized by one-sided finite differences [12, p. 1721] causing the tensor components below to become nonzero

$$
\begin{aligned}
&{}^{\underline{d},\frac{1}{2}}_{d,\beta}B^{1;1,\underline{q}}_{0;1,q}, \quad \beta = \tfrac{1}{2}\\
&{}^{\underline{d},\frac{1}{2}}_{d-1,1}B^{1;1,\underline{q}}_{0;j,q}, \quad j = m_{1,d-1}-3,\ldots,m_{1,d-1}\\
&{}^{\underline{d},\frac{1}{2}}_{d,1}B^{1;1,\underline{q}}_{0;j,q}, \quad j = 1,\ldots,4
\end{aligned}
$$

for $d = 2,\ldots,n$, $q = 2,\ldots,m_2-1$.

7.2.1 Hybrid interface condition

The interface condition (14) is reformulated as

$$
\frac{\varrho_n}{\varrho_{n+1}}\hbar_{1,n}\eta_{1,n}\frac{\partial p_{n+1}}{\partial n}(\xi_2) + \hbar_{1,n}\frac{\partial p_n}{\partial \xi_1}(n,\xi_2) = 0,
$$

where $\hbar_{1,n} = \frac{1}{m_{1,n}+1}$. The first term is discretized by collocating the approximant ${}^{n+1,\frac{1}{2}}p^1(\xi_2)$ to $\frac{\partial p_{n+1}}{\partial n}$. At the node points ξ_2^k, $k = 2,\ldots,m_2-1$, the second term is approximated by a fourth-order accurate finite difference formula based on function values at the grid points $(n - s\hbar_{1,n}, \xi_2^k)$, $s = 0,\ldots,4$. According to the elimination in Section 5.1, $p_n(n,\xi_2)$ is discretized by collocating the approximant ${}^{n+1,\frac{1}{2}}p^0(\xi_2)$. At collocation points separate from the node points, fourth-order accurate interpolation is utilized to approximate $p_n(n - s\hbar_{1,n}, \xi_2)$, $s = 1,\ldots,4$, which are required in the finite difference formula for $\frac{\partial p_n}{\partial \xi_1}(n,\xi_2)$ when $\xi_2 \neq \xi_2^k$.

Define the auxiliary quantities

$$
\begin{aligned}
h^{k,q} &\equiv \frac{\varrho_n}{\varrho_{n+1}}\hbar_{1,n}\eta_{1,n}\big(n, \xi_2^{k+\frac{q-1}{3}}\big), \qquad k = 2,\ldots,m_2-2, \quad q = 1,2,3,\\
h^{1,q} &\equiv \frac{\varrho_n}{\varrho_{n+1}}\hbar_{1,n}\eta_{1,n}\big(n, \xi_2^{\frac{3}{2}+\frac{q-1}{6}}\big), \qquad q = 2,3,\\
h^{m_2-1,q} &\equiv \frac{\varrho_n}{\varrho_{n+1}}\hbar_{1,n}\eta_{1,n}\big(n, \xi_2^{m_2-1+\frac{q-1}{6}}\big), \quad q = 1,2,3,
\end{aligned}
$$

evaluated at the indicated collocation points, and the finite difference weights

$$w_0 = \tfrac{25}{12}, \quad w_1 = -4, \quad w_2 = 3, \quad w_3 = -\tfrac{4}{3}, \quad w_4 = \tfrac{1}{4}.$$

The discretization of the reformulated interface condition contributes to the coefficient tensor B as described in the remainder of this section. At the node points indexed by $k = 2, \ldots, m_2 - 1$, the collocations yield

$${}^{n+1,\frac{1}{2}}_{n+1,\beta}B^{1;\underline{k},1}_{1;k-1,1} = h^{k,1}, \quad {}^{n+1,\frac{1}{2}}_{n+1,\beta}B^{1;\underline{k},1}_{0;k-1,1} = w_0, \quad \beta = \tfrac{1}{2},$$

and the finite difference yields

$${}^{n+1,\frac{1}{2}}_{n,1}B^{1;k,1}_{0;m_{1,n}-s,k} = w_{s+1}, \quad s = 0, \ldots, 3.$$

For $\beta = \frac{1}{2}$, the collocations at the points between the node points result in

$$\begin{aligned}
{}^{n+1,\frac{1}{2}}_{n+1,\beta}B^{1;\underline{k},2}_{1;k-1,1} &= \tfrac{2}{3}h^{k,2}, & {}^{n+1,\frac{1}{2}}_{n+1,\beta}B^{1;\underline{k},3}_{1;k-1,1} &= \tfrac{1}{3}h^{k,3}, & k &= 2, \ldots, m_2 - 1,\\
{}^{n+1,\frac{1}{2}}_{n+1,\beta}B^{1;\underline{k},2}_{1;k,1} &= \tfrac{1}{3}h^{k,2}, & {}^{n+1,\frac{1}{2}}_{n+1,\beta}B^{1;\underline{k},3}_{1;k,1} &= \tfrac{2}{3}h^{k,3}, & k &= 1, \ldots, m_2 - 2,\\
{}^{n+1,\frac{1}{2}}_{n+1,\beta}B^{1;\underline{k},2}_{1;k,2} &= -\tfrac{4}{9}h^{k,2}, & {}^{n+1,\frac{1}{2}}_{n+1,\beta}B^{1;\underline{k},3}_{1;k,2} &= -\tfrac{4}{9}h^{k,3}, & &\\
{}^{n+1,\frac{1}{2}}_{n+1,\beta}B^{1;\underline{k},2}_{1;k,3} &= \tfrac{4}{27}h^{k,2}, & {}^{n+1,\frac{1}{2}}_{n+1,\beta}B^{1;\underline{k},3}_{1;k,3} &= -\tfrac{4}{27}h^{k,3}, & k &= 1, \ldots, m_2 - 1,
\end{aligned}$$

$$\begin{aligned}
{}^{n+1,\frac{1}{2}}_{n+1,\beta}B^{1;\underline{k},2}_{0;k-1,1} &= \tfrac{2}{3}w_0, & {}^{n+1,\frac{1}{2}}_{n+1,\beta}B^{1;\underline{k},3}_{0;k-1,1} &= \tfrac{1}{3}w_0, & k &= 2, \ldots, m_2 - 1,\\
{}^{n+1,\frac{1}{2}}_{n+1,\beta}B^{1;\underline{k},2}_{0;k,1} &= \tfrac{1}{3}w_0, & {}^{n+1,\frac{1}{2}}_{n+1,\beta}B^{1;\underline{k},3}_{0;k,1} &= \tfrac{2}{3}w_0, & k &= 1, \ldots, m_2 - 2,\\
{}^{n+1,\frac{1}{2}}_{n+1,\beta}B^{1;\underline{k},2}_{0;k,2} &= -\tfrac{4}{9}w_0, & {}^{n+1,\frac{1}{2}}_{n+1,\beta}B^{1;\underline{k},3}_{0;k,2} &= -\tfrac{4}{9}w_0, & &\\
{}^{n+1,\frac{1}{2}}_{n+1,\beta}B^{1;\underline{k},2}_{0;k,3} &= \tfrac{4}{27}w_0, & {}^{n+1,\frac{1}{2}}_{n+1,\beta}B^{1;\underline{k},3}_{0;k,3} &= -\tfrac{4}{27}w_0, & k &= 1, \ldots, m_2 - 1,
\end{aligned}$$

and by interpolation from the four nearest grid points, the finite differences at the points between the node points result in

$$\begin{aligned}
{}^{n+1,\frac{1}{2}}_{n,1}B^{1;k,2}_{0;m_{1,n}-s,k-1} &= {}^{n+1,\frac{1}{2}}_{n,1}B^{1;k,3}_{0;m_{1,n}-s,k+2} = -\tfrac{5}{81}w_{s+1},\\
{}^{n+1,\frac{1}{2}}_{n,1}B^{1;k,2}_{0;m_{1,n}-s,k} &= {}^{n+1,\frac{1}{2}}_{n,1}B^{1;k,3}_{0;m_{1,n}-s,k+1} = \tfrac{20}{27}w_{s+1},\\
{}^{n+1,\frac{1}{2}}_{n,1}B^{1;k,2}_{0;m_{1,n}-s,k+1} &= {}^{n+1,\frac{1}{2}}_{n,1}B^{1;k,3}_{0;m_{1,n}-s,k} = \tfrac{10}{27}w_{s+1},\\
{}^{n+1,\frac{1}{2}}_{n,1}B^{1;k,2}_{0;m_{1,n}-s,k+2} &= {}^{n+1,\frac{1}{2}}_{n,1}B^{1;k,3}_{0;m_{1,n}-s,k-1} = -\tfrac{4}{81}w_{s+1}
\end{aligned}$$

for $k = 2, \ldots, m_2 - 2$, $s = 0, \ldots, 3$.

Elimination according to (28) and (27) leads to

$$
\begin{aligned}
{}^{n+1,\frac{1}{2}}_{n+1,0}B^{1;1,2}_{0;0,1} &= \frac{2}{3}\Big(\frac{h^{1,2}}{h_{0,n+1}} + w_0\Big), & {}^{n+1,\frac{1}{2}}_{n+1,0}B^{1;1,3}_{0;0,1} &= \frac{1}{3}\Big(\frac{h^{1,3}}{h_{0,n+1}} + w_0\Big),\\
{}^{n+1,\frac{1}{2}}_{n+1,0}B^{1;1,2}_{0;1,1} &= -\frac{2h^{1,2}}{3h_{0,n+1}}, & {}^{n+1,\frac{1}{2}}_{n+1,0}B^{1;1,3}_{0;1,1} &= -\frac{h^{1,3}}{3h_{0,n+1}},\\
{}^{n+1,\frac{1}{2}}_{n+1,0}B^{1;1,2}_{0;1,2} &= \frac{4h^{1,2}}{3h_{0,n+1}}, & {}^{n+1,\frac{1}{2}}_{n+1,0}B^{1;1,3}_{0;1,2} &= \frac{2h^{1,3}}{3h_{0,n+1}},\\
{}^{n+1,\frac{1}{2}}_{n+1,0}B^{1;1,2}_{0;1,3} &= -\frac{4h^{1,2}}{3h_{0,n+1}}, & {}^{n+1,\frac{1}{2}}_{n+1,0}B^{1;1,3}_{0;1,3} &= -\frac{2h^{1,3}}{3h_{0,n+1}},
\end{aligned}
$$

$$
\begin{aligned}
{}^{n+1,\frac{1}{2}}_{n+1,1}B^{1;m_2-1,2}_{0;0,1} &= \frac{1}{3}\Big(\frac{h^{m_2-1,2}}{h_{1,n+1}} + w_0\Big), & {}^{n+1,\frac{1}{2}}_{n+1,1}B^{1;m_2-1,3}_{0;0,1} &= \frac{2}{3}\Big(\frac{h^{m_2-1,3}}{h_{1,n+1}} + w_0\Big),\\
{}^{n+1,\frac{1}{2}}_{n+1,1}B^{1;m_2-1,2}_{0;1,1} &= -\frac{h^{m_2-1,2}}{3h_{1,n+1}}, & {}^{n+1,\frac{1}{2}}_{n+1,1}B^{1;m_2-1,3}_{0;1,1} &= -\frac{2h^{m_2-1,3}}{3h_{1,n+1}},\\
{}^{n+1,\frac{1}{2}}_{n+1,1}B^{1;m_2-1,2}_{0;1,2} &= \frac{2h^{m_2-1,2}}{3h_{1,n+1}}, & {}^{n+1,\frac{1}{2}}_{n+1,1}B^{1;m_2-1,3}_{0;1,2} &= \frac{4h^{m_2-1,3}}{3h_{1,n+1}},\\
{}^{n+1,\frac{1}{2}}_{n+1,1}B^{1;m_2-1,2}_{0;1,3} &= -\frac{2h^{m_2-1,2}}{3h_{1,n+1}}, & {}^{n+1,\frac{1}{2}}_{n+1,1}B^{1;m_2-1,3}_{0;1,3} &= -\frac{4h^{m_2-1,3}}{3h_{1,n+1}}.
\end{aligned}
$$

The interpolations required in the finite difference formula for the first two and last two collocation points give

$$
\begin{aligned}
{}^{n+1,\frac{1}{2}}_{n,1}B^{1;1,2}_{0;m_{1,n}-s,1} &= {}^{n+1,\frac{1}{2}}_{n,1}B^{1;m_2-1,3}_{0;m_{1,n}-s,m_2} &&= \tfrac{14}{81}w_{s+1},\\
{}^{n+1,\frac{1}{2}}_{n,1}B^{1;1,2}_{0;m_{1,n}-s,2} &= {}^{n+1,\frac{1}{2}}_{n,1}B^{1;m_2-1,3}_{0;m_{1,n}-s,m_2-1} &&= \tfrac{28}{27}w_{s+1},\\
{}^{n+1,\frac{1}{2}}_{n,1}B^{1;1,2}_{0;m_{1,n}-s,3} &= {}^{n+1,\frac{1}{2}}_{n,1}B^{1;m_2-1,3}_{0;m_{1,n}-s,m_2-2} &&= -\tfrac{7}{27}w_{s+1},\\
{}^{n+1,\frac{1}{2}}_{n,1}B^{1;1,2}_{0;m_{1,n}-s,4} &= {}^{n+1,\frac{1}{2}}_{n,1}B^{1;m_2-1,3}_{0;m_{1,n}-s,m_2-3} &&= \tfrac{4}{81}w_{s+1},
\end{aligned}
$$

$$
\begin{aligned}
{}^{n+1,\frac{1}{2}}_{n,1}B^{1;1,3}_{0;m_{1,n}-s,1} &= {}^{n+1,\frac{1}{2}}_{n,1}B^{1;m_2-1,2}_{0;m_{1,n}-s,m_2} &&= \tfrac{91}{1296}w_{s+1},\\
{}^{n+1,\frac{1}{2}}_{n,1}B^{1;1,3}_{0;m_{1,n}-s,2} &= {}^{n+1,\frac{1}{2}}_{n,1}B^{1;m_2-1,2}_{0;m_{1,n}-s,m_2-1} &&= \tfrac{455}{432}w_{s+1},\\
{}^{n+1,\frac{1}{2}}_{n,1}B^{1;1,3}_{0;m_{1,n}-s,3} &= {}^{n+1,\frac{1}{2}}_{n,1}B^{1;m_2-1,2}_{0;m_{1,n}-s,m_2-2} &&= -\tfrac{65}{432}w_{s+1},\\
{}^{n+1,\frac{1}{2}}_{n,1}B^{1;1,3}_{0;m_{1,n}-s,4} &= {}^{n+1,\frac{1}{2}}_{n,1}B^{1;m_2-1,2}_{0;m_{1,n}-s,m_2-3} &&= \tfrac{35}{1296}w_{s+1}
\end{aligned}
$$

for $s = 0, \ldots, 3$.

7.3 Compatibility conditions

Due to the labeling (described in Section 6.5) of the compatibility conditions, equations (29) subject to elimination according to (27) generate the following set of tensor components

$$
\begin{aligned}
{}^{\delta,0}_{\delta,\frac{1}{2}}B^{0;1,1}_{0;1,1} &= -1, \quad {}^{\delta,0}_{\delta,\frac{1}{2}}B^{0;1,1}_{0;1,2} = 2, \quad {}^{\delta,0}_{\delta,\frac{1}{2}}B^{0;1,1}_{0;1,3} = -2,\\
{}^{\delta,0}_{\delta,0}B^{0;1,1}_{0;0,1} &= 1, \quad {}^{\delta,0}_{\delta,0}B^{0;1,1}_{1;0,1} = -h^1_\delta \eta_{t,\delta}(0),
\end{aligned}
$$

$$
\begin{aligned}
{}^{\delta,1}_{\delta,\frac{1}{2}}B^{0;1,1}_{0;j-1,1} &= -1, \quad {}^{\delta,1}_{\delta,\frac{1}{2}}B^{0;1,1}_{0;j,2} = 2, \quad {}^{\delta,1}_{\delta,\frac{1}{2}}B^{0;1,1}_{0;j,3} = 2,\\
{}^{\delta,1}_{\delta,1}B^{0;1,1}_{0;0,1} &= 1, \quad {}^{\delta,1}_{\delta,1}B^{0;1,1}_{1;0,1} = -h^j_\delta \eta_{t,\delta}(1), \quad j = m_{\frac{1}{2},\delta},
\end{aligned}
$$

where $\delta = n+1, \ldots, N$.

7.4 Dirichlet-to-Neumann conditions

The DtN conditions (7) and (8) are collocated at points on the vertical boundaries. The assembly is performed in two steps. Firstly, we form the Dirichlet part corresponding to the expansion in the eigenfunctions. Secondly, for nodes in domains discretized by finite differences, we add the Neumann part corresponding to the normal derivative. For points in the BIE region, the coefficients for the approximants of the normal derivative are degrees of freedom, which implies that the Neumann part constitutes separate tensor components. The auxiliary tensors D and U are defined in Appendices A and B, respectively.

7.4.1 Dirichlet

In order to get a clearer description of the tensor components below, we first assemble the tensor W from the element-based tensor D.

For boundary label $b = 0, 1$ and mode index $m = 1, \ldots, \mu_b$; the components of W for domain index $\delta = n+1, \ldots, N$ become

$$
\begin{aligned}
{}^{b}_{\delta}W^{m}_{j,p} &= {}^{b}_{\delta}D^{m}_{j,p}, \quad j = 1, \ldots, m_{b,\delta}, \quad p = 2, 3,\\
{}^{b}_{\delta}W^{m}_{j,1} &= {}^{b}_{\delta}D^{m}_{j,4} + {}^{b}_{\delta}D^{m}_{j+1,1}, \quad j = 1, \ldots, m_{b,\delta} - 1;
\end{aligned}
$$

and the contributions pertaining to nodal basis polynomials with support at interface nodes are given by

$$
\begin{aligned}
{}^{b}_{n+1}W^{m}_{0,1} &= {}^{b}_{n+1}D^{m}_{1,1} + {}_{n+1,b}U^{0;1,1}_{0;0,1}\, {}^{n+1}_{b}\Psi^{1,1}_{m},\\
{}^{b}_{\delta}W^{m}_{0,1} &= {}^{b}_{\delta}D^{m}_{1,1} + {}^{b}_{\delta-1}D^{m}_{m_{b,\delta-1},4}, \quad \delta = n+2, \ldots, N\\
({}^{b}_{N}W^{m}_{m_{b,N},1} &= {}^{b}_{N}D^{m}_{m_{b,N},4}).
\end{aligned}
$$

Note that all the formulas below come in pairs corresponding to the two DtN conditions. The reason for there being nine pairs of equations is that there are interactions between three types of points. There are nodes on the interfaces between the top n layers, nodes interior to the top n layers, and BIE points. The range of index j is inherited either from that of U or W.

Collocation on the interfaces between the top n layers indexed by $d = 2, \ldots, n$ yields

$$
\begin{aligned}
{}^{d,\frac{1}{2}}_{\delta,\beta}B^{1;1,1}_{0;1,p} &= C^0_m \, {}^d_0\Psi_m \, {}^0_\delta[\Psi^T]^m \, {}_{\delta,\beta}U^{0;1,1}_{0;1,p}, \qquad p = 1, \ldots, 4, \\
{}^{d,\frac{1}{2}}_{\delta,\beta}B^{1;1,m_2}_{0;1,p} &= C^1_m \, {}^d_1\Psi_m \, {}^1_\delta[\Psi^T]^m \, {}_{\delta,\beta}U^{0;1,m_2}_{0;1,p}, \quad p = m_2 - 3, \ldots, m_2
\end{aligned}
$$

for $\delta = 2, \ldots, n$, $\beta = \frac{1}{2}$, and

$$
\begin{aligned}
{}^{d,\frac{1}{2}}_{\delta,1}B^{1;1,1}_{0;j,p} &= C^0_m \, {}^d_0\Psi_m \, {}^0_\delta[\Psi^T]^m_\ell \, {}_{\delta,1}U^{0;\ell,1}_{0;j,p}, \qquad p = 1, 2, \\
{}^{d,\frac{1}{2}}_{\delta,1}B^{1;1,m_2}_{0;j,p} &= C^1_m \, {}^d_1\Psi_m \, {}^1_\delta[\Psi^T]^m_\ell \, {}_{\delta,1}U^{0;\ell,m_2}_{0;j,p}, \quad p = m_2 - 1, m_2
\end{aligned}
$$

for $\delta = 1, \ldots, n$, and

$$
\left.
\begin{aligned}
{}^{d,\frac{1}{2}}_{\delta,0}B^{1;1,1}_{0;j,p} &= C^0_m \, {}^d_0\Psi_m \, {}^0_\delta W^m_{j,p} \\
{}^{d,\frac{1}{2}}_{\delta,1}B^{1;1,m_2}_{0;j,p} &= C^1_m \, {}^d_1\Psi_m \, {}^1_\delta W^m_{j,p}
\end{aligned}
\right., \quad p = 1, 2, 3
$$

for $\delta = n + 1, \ldots, N$.

Collocation at points interior to the top n layers indexed by $d = 1, \ldots, n$, $k = 1, \ldots, m_{1,d}$ yields

$$
\begin{aligned}
{}^{d,1}_{\delta,\frac{1}{2}}B^{1;k,1}_{0;1,p} &= C^0_m \, {}^d_0\Psi^k_m \, {}^0_\delta[\Psi^T]^m \, {}_{\delta,\frac{1}{2}}U^{0;1,1}_{0;1,p}, \qquad p = 1, \ldots, 4, \\
{}^{d,1}_{\delta,\frac{1}{2}}B^{1;k,m_2}_{0;1,p} &= C^1_m \, {}^d_1\Psi^k_m \, {}^1_\delta[\Psi^T]^m \, {}_{\delta,\frac{1}{2}}U^{0;1,m_2}_{0;1,p}, \quad p = m_2 - 3, \ldots, m_2
\end{aligned}
$$

for $\delta = 2, \ldots, n$, and

$$
\begin{aligned}
{}^{d,1}_{\delta,1}B^{1;k,1}_{0;j,p} &= C^0_m \, {}^d_0\Psi^k_m \, {}^0_\delta[\Psi^T]^m_\ell \, {}_{\delta,1}U^{0;\ell,1}_{0;j,p}, \qquad p = 1, 2, \\
{}^{d,1}_{\delta,1}B^{1;k,m_2}_{0;j,p} &= C^1_m \, {}^d_1\Psi^k_m \, {}^1_\delta[\Psi^T]^m_\ell \, {}_{\delta,1}U^{0;\ell,m_2}_{0;j,p}, \quad p = m_2 - 1, m_2
\end{aligned}
$$

for $\delta = 1, \ldots, n$, and

$$
\left.
\begin{aligned}
{}^{d,1}_{\delta,0}B^{1;k,1}_{0;j,p} &= C^0_m \, {}^d_0\Psi^k_m \, {}^0_\delta W^m_{j,p} \\
{}^{d,1}_{\delta,1}B^{1;k,m_2}_{0;j,p} &= C^1_m \, {}^d_1\Psi^k_m \, {}^1_\delta W^m_{j,p}
\end{aligned}
\right., \quad p = 1, 2, 3
$$

for $\delta = n + 1, \ldots, N$.

Collocation at BIE points indexed by $d = n+1, \dots, N$, $k = 1, \dots, m_{b,d}$, $q = 1, 2, 3$ yields

$$
\begin{aligned}
{}^{d,0}_{\delta,\frac{1}{2}}B^{1;k,q}_{0;1,p} &= C^{0}_{m}\,{}^{d}_{0}\Psi^{k,q}_{m}\,{}^{0}_{\delta}[\Psi^{T}]^{m}\,{}_{\delta,\frac{1}{2}}U^{0;1,1}_{0;1,p}, && p = 1, \dots, 4,\\
{}^{d,1}_{\delta,\frac{1}{2}}B^{1;k,q}_{0;1,p} &= C^{1}_{m}\,{}^{d}_{1}\Psi^{k,q}_{m}\,{}^{1}_{\delta}[\Psi^{T}]^{m}\,{}_{\delta,\frac{1}{2}}U^{0;1,m_2}_{0;1,p}, && p = m_2 - 3, \dots, m_2
\end{aligned}
$$

for $\delta = 2, \dots, n$, and

$$
\begin{aligned}
{}^{d,0}_{\delta,1}B^{1;k,q}_{0;j,p} &= C^{0}_{m}\,{}^{d}_{0}\Psi^{k,q}_{m}\,{}^{0}_{\delta}[\Psi^{T}]^{m}_{\ell}\,{}_{\delta,1}U^{0;\ell,1}_{0;j,p}, && p = 1, 2,\\
{}^{d,1}_{\delta,1}B^{1;k,q}_{0;j,p} &= C^{1}_{m}\,{}^{d}_{1}\Psi^{k,q}_{m}\,{}^{1}_{\delta}[\Psi^{T}]^{m}_{\ell}\,{}_{\delta,1}U^{0;\ell,m_2}_{0;j,p}, && p = m_2 - 1, m_2
\end{aligned}
$$

for $\delta = 1, \dots, n$, and

$$
\left.
\begin{aligned}
{}^{d,0}_{\delta,0}B^{1;k,q}_{0;j,p} &= C^{0}_{m}\,{}^{d}_{0}\Psi^{k,q}_{m}\,{}^{0}_{\delta}W^{m}_{j,p}\\
{}^{d,1}_{\delta,1}B^{1;k,q}_{0;j,p} &= C^{1}_{m}\,{}^{d}_{1}\Psi^{k,q}_{m}\,{}^{1}_{\delta}W^{m}_{j,p}
\end{aligned}
\right., \quad p = 1, 2, 3
$$

for $\delta = n + 1, \dots, N$.

7.4.2 Neumann

At every collocation point on the interfaces between the top n layers, the normal derivative (w.r.t. the vertical boundaries) is discretized by a finite difference formula involving the nearest five nodes along the interface. This leads to the following updates for $d = 2, \dots, n$, $b = \frac{1}{2}$,

$$
\begin{aligned}
{}^{\underline{d},b}_{d,\frac{1}{2}}B^{1;1,1}_{0;1,p} &\overset{+}{\leftarrow} {}_{d,\frac{1}{2}}U^{1;1,1}_{0;1,p}, && p = 1, \dots, 5,\\
{}^{\underline{d},b}_{d,\frac{1}{2}}B^{1;1,m_2}_{0;1,p} &\overset{+}{\leftarrow} {}_{d,\frac{1}{2}}U^{1;1,m_2}_{0;1,p}, && p = m_2 - 4, \dots, m_2,
\end{aligned}
$$

where $\overset{+}{\leftarrow}$ denotes addition to the left-hand side.

At the collocation points interior to the top n layers, the six-point Numerov approximation in Appendix B is used, leading to couplings of some interior points and interface nodes. The resulting updates become:

for $d = 1, \dots, n$, $k = 1, \dots, m_{1,d}$, $j = k - 1, k, k + 1$,

$$
\begin{aligned}
{}^{\underline{d},1}_{d,1}B^{1;k,1}_{0;j,p} &\overset{+}{\leftarrow} {}_{d,1}U^{1;k,1}_{0;j,p}, && p = 1, 2,\\
{}^{\underline{d},1}_{d,1}B^{1;k,m_2}_{0;j,p} &\overset{+}{\leftarrow} {}_{d,1}U^{1;k,m_2}_{0;j,p}, && p = m_2 - 1, m_2,
\end{aligned}
$$

where $j \neq 0, m_{1,d} + 1$, i.e., excluding the couplings to interface nodes;

for $d = 2, \dots, n$,

$$
\begin{aligned}
{}^{\underline{d},1}_{d,\frac{1}{2}}B^{1;1,1}_{0;1,p} &\overset{+}{\leftarrow} {}_{d,1}U^{1;1,1}_{0;0,p}, && p = 1, 2,\\
{}^{\underline{d},1}_{d,\frac{1}{2}}B^{1;1,m_2}_{0;1,p} &\overset{+}{\leftarrow} {}_{d,1}U^{1;1,m_2}_{0;0,p}, && p = m_2 - 1, m_2,
\end{aligned}
$$

including the couplings to nodes on the "top" interfaces;

for $d = 1, \ldots, n-1$,

$$
\begin{aligned}
{}^{\underline{d},1}_{d+1,\frac{1}{2}}B^{1;m_{1,d},1}_{0;1,p} &\overset{+}{\leftarrow} {}_{d,1}U^{1;m_{1,d},1}_{0;m_{1,d}+1,p}, \quad p = 1, 2, \\
{}^{\underline{d},1}_{d+1,\frac{1}{2}}B^{1;m_{1,d},m_2}_{0;1,p} &\overset{+}{\leftarrow} {}_{d,1}U^{1;m_{1,d},m_2}_{0;m_{1,d}+1,p}, \quad p = m_2 - 1, m_2,
\end{aligned}
$$

$$
\begin{aligned}
{}^{n,1}_{n+1,0}B^{1;m_{1,n},1}_{0;0,1} &\overset{+}{\leftarrow} {}_{n,1}U^{1;m_{1,n},1}_{0;m_{1,n}+1,2}, & {}^{n,1}_{n+1,0}B^{1;m_{1,n},1}_{1;0,1} &= {}_{n,1}U^{1;m_{1,n},1}_{0;m_{1,n}+1,1}, \\
{}^{n,1}_{n+1,1}B^{1;m_{1,n},m_2}_{0;0,1} &\overset{+}{\leftarrow} {}_{n,1}U^{1;m_{1,n},m_2}_{0;m_{1,n}+1,m_2-1}, & {}^{n,1}_{n+1,1}B^{1;m_{1,n},m_2}_{1;0,1} &= {}_{n,1}U^{1;m_{1,n},m_2}_{0;m_{1,n}+1,m_2},
\end{aligned}
$$

including the couplings to nodes on the "bottom" interfaces.

For the BIE collocation points, the basis functions representing the normal derivative are simply evaluated. For $b = 0, 1$, $d = n{+}1, \ldots, N$, the resulting components are

$$
\begin{aligned}
& & {}^{\underline{d,b}}_{d,b}B^{1;\underline{k},2}_{1;k,2} &= -\tfrac{4}{9}, & {}^{\underline{d,b}}_{d,b}B^{1;\underline{k},3}_{1;k,2} &= -\tfrac{4}{9}, & \\
& & {}^{\underline{d,b}}_{d,b}B^{1;\underline{k},2}_{1;k,3} &= \tfrac{4}{27}, & {}^{\underline{d,b}}_{d,b}B^{1;\underline{k},3}_{1;k,3} &= -\tfrac{4}{27}, & \\
{}^{\underline{d,b}}_{d,b}B^{1;\underline{k},1}_{1;k-1,1} &= 1, & {}^{\underline{d,b}}_{d,b}B^{1;\underline{k},2}_{1;k-1,1} &= \tfrac{2}{3}, & {}^{\underline{d,b}}_{d,b}B^{1;\underline{k},3}_{1;k-1,1} &= \tfrac{1}{3}, & k &= 1, \ldots, m_{b,d}, \\
& & {}^{\underline{d,b}}_{d,b}B^{1;\underline{k},2}_{1;k,1} &= \tfrac{1}{3}, & {}^{\underline{d,b}}_{d,b}B^{1;\underline{k},3}_{1;k,1} &= \tfrac{2}{3}, & k &= 1, \ldots, m_{b,d} - 1,
\end{aligned}
$$

and, due to elimination according to (25),

$$
{}^{\underline{d,b}}_{d+1,b}B^{1;m_{b,d},2}_{1;0,1} = \tfrac{1}{3}, \qquad {}^{\underline{d,b}}_{d+1,b}B^{1;m_{b,d},3}_{1;0,1} = \tfrac{2}{3}, \qquad b = 0, 1, \quad d = n+1, \ldots, N-1.
$$

7.5 Boundary integral equations

This section contains the description of the tensor components coming from BIEs (19), (20) collocated at points ${}^{d,b}x_1^{k,q}$ ($b = 0, 1$) and BIEs (21), (22) collocated at ${}^{d}t^{k,q}$ ($b = \frac{1}{2}$), where $k = 1, \ldots, m_{b,d}$, $q = 1, 2, 3$ excluding the combination $k = 1$ and $q = 1$. Default index ranges for the unknowns are $\beta = 0, \frac{1}{2}, 1$, $\iota = 0, 1$.

7.5.1 Collocation at the vertical boundaries and the top interfaces

Consider the contributions from (19–21), i.e., collocation on the vertical boundaries and on the top interfaces labeled $b = 0, 1, \frac{1}{2}$, $d = n+1, \ldots, N$.

Firstly, the contributions caused by the integrals $I_{d,\beta}$ in equations (17,15,18) are treated. The corresponding element integrals yield these tensor components

$$
{}^{\underline{d,b}}_{d,\beta}B^{0;k,q}_{\iota;j,1} = {}^{d,b}_{\ \beta}A^{0;k,q}_{\iota;j,4} + {}^{d,b}_{\ \beta}A^{0;k,q}_{\iota;j+1,1}, \quad j = 1, \ldots, m_{\beta,d} - 1,
$$

pertaining to nodal (linear) basis polynomials, and

$$ {}^{\underline{d},b}_{d,\beta}B^{0;k,q}_{\iota;j,p} = {}^{d,b}_{\ \beta}A^{0;k,q}_{\iota;j,p}, \quad j = 1, \ldots, m_{\beta,d}, \quad p = 2, 3, $$

pertaining to higher degree basis polynomials.

For $\beta = 0, 1$, the tensor components pertaining to corner nodal basis polynomials are

$$ {}^{\underline{d},b}_{d,\beta}B^{0;k,q}_{\iota;0,1} = {}^{d,b}_{\ \beta}A^{0;k,q}_{\iota;1,1}, $$

and, due to elimination according to (25),

$$ {}^{\underline{d},b}_{d+1,\beta}B^{0;k,q}_{\iota;0,1} = {}^{d,b}_{\ \beta}A^{0;k,q}_{\iota;j,4}, \quad d = n+1, \ldots, N-1, \quad j = m_{\beta,d}. $$

The following updates are due to elimination according to (27)

$$ \begin{aligned} {}^{\underline{d},b}_{d,0}B^{0;k,q}_{0;0,1} &\stackrel{+}{\leftarrow} {}^{d,b}_{\ \frac{1}{2}}A^{0;k,q}_{0;1,1}, \\ {}^{\underline{d},b}_{d,1}B^{0;k,q}_{0;0,1} &\stackrel{+}{\leftarrow} {}^{d,b}_{\ \frac{1}{2}}A^{0;k,q}_{0;j,4}, \quad j = m_{\frac{1}{2},d}, \end{aligned} $$

and (28)

$$ \begin{aligned} {}^{\underline{d},b}_{d,0}B^{0;k,q}_{0;0,1} &\stackrel{+}{\leftarrow} \tfrac{1}{h_{0,d}}\, {}^{d,b}_{\ \frac{1}{2}}A^{0;k,q}_{1;1,1}, & {}^{\underline{d},b}_{d,0}B^{0;k,q}_{0;1,1} &\stackrel{+}{\leftarrow} -\tfrac{1}{h_{0,d}}\, {}^{d,b}_{\ \frac{1}{2}}A^{0;k,q}_{1;1,1}, \\ {}^{\underline{d},b}_{d,0}B^{0;k,q}_{0;1,2} &\stackrel{+}{\leftarrow} \tfrac{2}{h_{0,d}}\, {}^{d,b}_{\ \frac{1}{2}}A^{0;k,q}_{1;1,1}, & {}^{\underline{d},b}_{d,0}B^{0;k,q}_{0;1,3} &\stackrel{+}{\leftarrow} -\tfrac{2}{h_{0,d}}\, {}^{d,b}_{\ \frac{1}{2}}A^{0;k,q}_{1;1,1}, \\ {}^{\underline{d},b}_{d,1}B^{0;k,q}_{0;0,1} &\stackrel{+}{\leftarrow} \tfrac{1}{h_{1,d}}\, {}^{d,b}_{\ \frac{1}{2}}A^{0;k,q}_{1;j,4}, & {}^{\underline{d},b}_{d,1}B^{0;k,q}_{0;1,1} &\stackrel{+}{\leftarrow} -\tfrac{1}{h_{1,d}}\, {}^{d,b}_{\ \frac{1}{2}}A^{0;k,q}_{1;j,4}, \\ {}^{\underline{d},b}_{d,1}B^{0;k,q}_{0;1,2} &\stackrel{+}{\leftarrow} \tfrac{2}{h_{1,d}}\, {}^{d,b}_{\ \frac{1}{2}}A^{0;k,q}_{1;j,4}, & {}^{\underline{d},b}_{d,1}B^{0;k,q}_{0;1,3} &\stackrel{+}{\leftarrow} -\tfrac{2}{h_{1,d}}\, {}^{d,b}_{\ \frac{1}{2}}A^{0;k,q}_{1;j,4}, \quad j = m_{\frac{1}{2},d}. \end{aligned} $$

Secondly, the contributions caused by the integrals $I_{d,\frac{3}{2}}$ in (16a) are treated. The corresponding element integrals yield these tensor components

$$ {}^{\underline{d},b}_{d+1,\frac{1}{2}}B^{0;k,q}_{\iota;j,1} = {}^{d,b}_{\ \frac{3}{2}}A^{0;k,q}_{\iota;j,4} + {}^{d,b}_{\ \frac{3}{2}}A^{0;k,q}_{\iota;j+1,1}, \quad j = 1, \ldots, m_{\frac{1}{2},d+1} - 1, $$

pertaining to nodal (linear) basis polynomials, and

$$ {}^{\underline{d},b}_{d+1,\frac{1}{2}}B^{0;k,q}_{\iota;j,p} = {}^{d,b}_{\ \frac{3}{2}}A^{0;k,q}_{\iota;j,p}, \quad j = 1, \ldots, m_{\frac{1}{2},d+1}, \quad p = 2, 3, $$

pertaining to higher degree basis polynomials, with the understanding that components with subindex $d+1 = N+1$ are redundant.

The following updates are due to elimination according to (27)

$$ \begin{aligned} {}^{\underline{d},b}_{d+1,0}B^{0;k,q}_{0;0,1} &\stackrel{+}{\leftarrow} {}^{d,b}_{\ \frac{3}{2}}A^{0;k,q}_{0;1,1}, \\ {}^{\underline{d},b}_{d+1,1}B^{0;k,q}_{0;0,1} &\stackrel{+}{\leftarrow} {}^{d,b}_{\ \frac{3}{2}}A^{0;k,q}_{0;j,4}, \quad j = m_{\frac{1}{2},d+1}, \end{aligned} $$

and (28)

$$
\begin{aligned}
&{}^{\underline{d},b}_{d+1,0}B^{0;k,q}_{0;0,1} \overset{+}{\leftarrow} \frac{1}{h_{0,d+1}}\,{}^{d,b}_{\frac{3}{2}}A^{0;k,q}_{1;1,1}, &\quad &{}^{\underline{d},b}_{d+1,0}B^{0;k,q}_{0;1,1} = -\frac{1}{h_{0,d+1}}\,{}^{d,b}_{\frac{3}{2}}A^{0;k,q}_{1;1,1},\\
&{}^{\underline{d},b}_{d+1,0}B^{0;k,q}_{0;1,2} = \frac{2}{h_{0,d+1}}\,{}^{d,b}_{\frac{3}{2}}A^{0;k,q}_{1;1,1}, &\quad &{}^{\underline{d},b}_{d+1,0}B^{0;k,q}_{0;1,3} = -\frac{2}{h_{0,d+1}}\,{}^{d,b}_{\frac{3}{2}}A^{0;k,q}_{1;1,1},\\
&{}^{\underline{d},b}_{d+1,1}B^{0;k,q}_{0;0,1} \overset{+}{\leftarrow} \frac{1}{h_{1,d+1}}\,{}^{d,b}_{\frac{3}{2}}A^{0;k,q}_{1;j,4}, &\quad &{}^{\underline{d},b}_{d+1,1}B^{0;k,q}_{0;1,1} = -\frac{1}{h_{1,d+1}}\,{}^{d,b}_{\frac{3}{2}}A^{0;k,q}_{1;j,4},\\
&{}^{\underline{d},b}_{d+1,1}B^{0;k,q}_{0;1,2} = \frac{2}{h_{1,d+1}}\,{}^{d,b}_{\frac{3}{2}}A^{0;k,q}_{1;j,4}, &\quad &{}^{\underline{d},b}_{d+1,1}B^{0;k,q}_{0;1,3} = -\frac{2}{h_{1,d+1}}\,{}^{d,b}_{\frac{3}{2}}A^{0;k,q}_{1;j,4}, \quad j = m_{\frac{1}{2},d+1}.
\end{aligned}
$$

For $e = 0$, collocation of the pressure term in (19–21) yields

(30a)
$$
\begin{aligned}
&{}^{\underline{d},\underline{b}}_{d,b}B^{e;j,2}_{0;\underline{j},1} \overset{+}{\leftarrow} \tfrac{1}{6}, \quad {}^{\underline{d},\underline{b}}_{d,b}B^{e;j,3}_{0;\underline{j},1} \overset{+}{\leftarrow} \tfrac{1}{3},\\
&{}^{\underline{d},\underline{b}}_{d,b}B^{e;j+1,1}_{0;\underline{j},1} \overset{+}{\leftarrow} \tfrac{1}{2}, \quad {}^{\underline{d},\underline{b}}_{d,b}B^{e;j+1,2}_{0;\underline{j},1} \overset{+}{\leftarrow} \tfrac{1}{3}, \quad {}^{\underline{d},\underline{b}}_{d,b}B^{e;j+1,3}_{0;\underline{j},1} \overset{+}{\leftarrow} \tfrac{1}{6}, \quad j = 1,\ldots,m_{b,d}-1,
\end{aligned}
$$

and

(30b)
$$
\begin{aligned}
&{}^{\underline{d},\underline{b}}_{d,b}B^{e;\underline{k},2}_{0;k,2} \overset{+}{\leftarrow} -\tfrac{2}{9}, \quad {}^{\underline{d},\underline{b}}_{d,b}B^{e;\underline{k},3}_{0;k,2} \overset{+}{\leftarrow} -\tfrac{2}{9},\\
&{}^{\underline{d},\underline{b}}_{d,b}B^{e;\underline{k},2}_{0;k,3} \overset{+}{\leftarrow} \tfrac{2}{27}, \quad {}^{\underline{d},\underline{b}}_{d,b}B^{e;\underline{k},3}_{0;k,3} \overset{+}{\leftarrow} -\tfrac{2}{27},
\end{aligned}
$$

and

$$
{}^{\underline{d},\underline{b}}_{d,b}B^{0;1,2}_{0;0,1} \overset{+}{\leftarrow} \tfrac{1}{3}, \qquad {}^{\underline{d},\underline{b}}_{d,b}B^{0;1,3}_{0;0,1} \overset{+}{\leftarrow} \tfrac{1}{6}, \quad b = 0,1,
$$

and, due to (25),

$$
{}^{\underline{d},\underline{b}}_{d+1,b}B^{0;m_{b,d},2}_{0;0,1} \overset{+}{\leftarrow} \tfrac{1}{6}, \quad {}^{\underline{d},\underline{b}}_{d+1,b}B^{0;m_{b,d},3}_{0;0,1} \overset{+}{\leftarrow} \tfrac{1}{3}, \quad b = 0,1, \quad d = n+1,\ldots,N-1,
$$

and, due to (27),

(30c)
$$
{}^{\underline{d},\frac{1}{2}}_{d,0}B^{e;1,2}_{0;0,1} \overset{+}{\leftarrow} \tfrac{1}{3}, \quad {}^{\underline{d},\frac{1}{2}}_{d,0}B^{e;1,3}_{0;0,1} \overset{+}{\leftarrow} \tfrac{1}{6},
$$

(30d)
$$
{}^{\underline{d},\frac{1}{2}}_{d,1}B^{e;k,2}_{0;0,1} \overset{+}{\leftarrow} \tfrac{1}{6}, \quad {}^{\underline{d},\frac{1}{2}}_{d,1}B^{e;k,3}_{0;0,1} \overset{+}{\leftarrow} \tfrac{1}{3}, \quad k = m_{\frac{1}{2},d}.
$$

7.5.2 Collocation at the bottom interfaces

Consider the contributions from (22), i.e., collocation on the bottom interfaces labeled $b = \frac{1}{2}$, $d = n+2,\ldots,N$.

Firstly, the contributions caused by the integrals $I_{d-1,\beta}$ in equations (17,15,18) are treated. The corresponding element integrals yield these tensor components

$$
{}^{\underline{d},\frac{1}{2}}_{d-1,\beta}B^{1;k,q}_{\iota;j,1} = {}^{d,\frac{1}{2}}_{\beta}A^{1;k,q}_{\iota;j,4} + {}^{d,\frac{1}{2}}_{\beta}A^{1;k,q}_{\iota;j+1,1}, \quad j = 1,\ldots,m_{\beta,d-1}-1,
$$

pertaining to nodal (linear) basis polynomials, and

$$
{}^{\underline{d},\frac{1}{2}}_{d-1,\beta}B^{1;k,q}_{\iota;j,p} = {}^{d,\frac{1}{2}}_{\beta}A^{1;k,q}_{\iota;j,p}, \quad j = 1,\ldots,m_{\beta,d-1}, \quad p = 2,3,
$$

pertaining to higher degree basis polynomials.

For $\beta = 0, 1$, the tensor components pertaining to corner nodal basis polynomials are

$$ {}^{\underline{d},\frac{1}{2}}_{d-1,\beta}B^{1;k,q}_{\iota;0,1} = {}^{d,\frac{1}{2}}_{\beta}A^{1;k,q}_{\iota;1,1}, $$

and, due to elimination according to (25),

$$ {}^{\underline{d},\frac{1}{2}}_{d,\beta}B^{1;k,q}_{\iota;0,1} = {}^{d,\frac{1}{2}}_{\beta}A^{1;k,q}_{\iota;j,4}, \quad j = m_{\beta,d-1}. $$

The following updates are due to elimination according to (27)

$$ \begin{aligned} &{}^{\underline{d},b}_{d-1,0}B^{1;k,q}_{0;0,1} \stackrel{+}{\leftarrow} {}^{d,b}_{\frac{1}{2}}A^{1;k,q}_{0;1,1}, \\ &{}^{\underline{d},b}_{d-1,1}B^{1;k,q}_{0;0,1} \stackrel{+}{\leftarrow} {}^{d,b}_{\frac{1}{2}}A^{1;k,q}_{0;j,4}, \quad j = m_{\frac{1}{2},d-1}, \end{aligned} $$

and (28)

$$ \begin{aligned} &{}^{\underline{d},b}_{d-1,0}B^{1;k,q}_{0;0,1} \stackrel{+}{\leftarrow} \frac{1}{h_{0,d-1}}\,{}^{d,b}_{\frac{1}{2}}A^{1;k,q}_{1;1,1}, \quad &&{}^{\underline{d},b}_{d-1,0}B^{1;k,q}_{0;1,1} \stackrel{+}{\leftarrow} -\frac{1}{h_{0,d-1}}\,{}^{d,b}_{\frac{1}{2}}A^{1;k,q}_{1;1,1}, \\ &{}^{\underline{d},b}_{d-1,0}B^{1;k,q}_{0;1,2} \stackrel{+}{\leftarrow} \frac{2}{h_{0,d-1}}\,{}^{d,b}_{\frac{1}{2}}A^{1;k,q}_{1;1,1}, \quad &&{}^{\underline{d},b}_{d-1,0}B^{1;k,q}_{0;1,3} \stackrel{+}{\leftarrow} -\frac{2}{h_{0,d-1}}\,{}^{d,b}_{\frac{1}{2}}A^{1;k,q}_{1;1,1}, \\ &{}^{\underline{d},b}_{d-1,1}B^{1;k,q}_{0;0,1} \stackrel{+}{\leftarrow} \frac{1}{h_{1,d-1}}\,{}^{d,b}_{\frac{1}{2}}A^{1;k,q}_{1;j,4}, \quad &&{}^{\underline{d},b}_{d-1,1}B^{1;k,q}_{0;1,1} \stackrel{+}{\leftarrow} -\frac{1}{h_{1,d-1}}\,{}^{d,b}_{\frac{1}{2}}A^{1;k,q}_{1;j,4}, \\ &{}^{\underline{d},b}_{d-1,1}B^{1;k,q}_{0;1,2} \stackrel{+}{\leftarrow} \frac{2}{h_{1,d-1}}\,{}^{d,b}_{\frac{1}{2}}A^{1;k,q}_{1;j,4}, \quad &&{}^{\underline{d},b}_{d-1,1}B^{1;k,q}_{0;1,3} \stackrel{+}{\leftarrow} -\frac{2}{h_{1,d-1}}\,{}^{d,b}_{\frac{1}{2}}A^{1;k,q}_{1;j,4}, \quad j = m_{\frac{1}{2},d-1}. \end{aligned} $$

Secondly, the contributions caused by the integrals $I_{d-1,\frac{3}{2}}$ in (16a) are treated. The corresponding element integrals yield these tensor components

$$ {}^{\underline{d},b}_{d,\frac{1}{2}}B^{1;k,q}_{\iota;j,1} = {}^{d,b}_{\frac{3}{2}}A^{1;k,q}_{\iota;j,4} + {}^{d,b}_{\frac{3}{2}}A^{1;k,q}_{\iota;j+1,1}, \quad j = 1, \ldots, m_{\frac{1}{2},d} - 1, $$

pertaining to nodal (linear) basis polynomials, and

$$ {}^{\underline{d},b}_{d,\frac{1}{2}}B^{1;k,q}_{\iota;j,p} = {}^{d,b}_{\frac{3}{2}}A^{1;k,q}_{\iota;j,p}, \quad j = 1, \ldots, m_{\frac{1}{2},d}, \quad p = 2, 3, $$

pertaining to higher degree basis polynomials.

The following updates are due to elimination according to (27)

$$ \begin{aligned} &{}^{\underline{d},b}_{d,0}B^{1;k,q}_{0;0,1} \stackrel{+}{\leftarrow} {}^{d,b}_{\frac{3}{2}}A^{1;k,q}_{0;1,1}, \\ &{}^{\underline{d},b}_{d,1}B^{1;k,q}_{0;0,1} \stackrel{+}{\leftarrow} {}^{d,b}_{\frac{3}{2}}A^{1;k,q}_{0;j,4}, \quad j = m_{\frac{1}{2},d}, \end{aligned} $$

and (28)

$$
\begin{aligned}
&{}^{d,b}_{d,0}B^{1;k,q}_{0;0,1} \xleftarrow{+} \tfrac{1}{h_{0,d}}\,{}^{d,b}_{\frac{3}{2}}A^{1;k,q}_{1;1,1}, && {}^{d,b}_{d,0}B^{1;k,q}_{0;1,1} = -\tfrac{1}{h_{0,d}}\,{}^{d,b}_{\frac{3}{2}}A^{1;k,q}_{1;1,1},\\
&{}^{d,b}_{d,0}B^{1;k,q}_{0;1,2} = \tfrac{2}{h_{0,d}}\,{}^{d,b}_{\frac{3}{2}}A^{1;k,q}_{1;1,1}, && {}^{d,b}_{d,0}B^{1;k,q}_{0;1,3} = -\tfrac{2}{h_{0,d}}\,{}^{d,b}_{\frac{3}{2}}A^{1;k,q}_{1;1,1},\\
&{}^{d,b}_{d,1}B^{1;k,q}_{0;0,1} \xleftarrow{+} \tfrac{1}{h_{1,d}}\,{}^{d,b}_{\frac{3}{2}}A^{1;k,q}_{1;j,4}, && {}^{d,b}_{d,1}B^{1;k,q}_{0;1,1} = -\tfrac{1}{h_{1,d}}\,{}^{d,b}_{\frac{3}{2}}A^{1;k,q}_{1;j,4},\\
&{}^{d,b}_{d,1}B^{1;k,q}_{0;1,2} = \tfrac{2}{h_{1,d}}\,{}^{d,b}_{\frac{3}{2}}A^{1;k,q}_{1;j,4}, && {}^{d,b}_{d,1}B^{1;k,q}_{0;1,3} = -\tfrac{2}{h_{1,d}}\,{}^{d,b}_{\frac{3}{2}}A^{1;k,q}_{1;j,4}, \qquad j = m_{\frac{1}{2},d}.
\end{aligned}
$$

The contributions from the collocation of the pressure term in (22) are given by formulas (30) for $e = 1$, $b = \frac{1}{2}$, $d = n+2, \ldots, N$.

A Appendix

The element integrals arising for the DtN conditions are given by

$$
{}^{b}_{\delta}D^{m}_{j,p} = \int\limits_{{}^{\delta,b}x_1^{j-1}}^{{}^{\delta,b}x_1^{j}} \frac{1}{\varrho_\delta}\widetilde{\psi}^{b}_{m}(x_1)\varphi_{j,p}(x_1)\,dx_1,
$$

where $b = 0, 1$, $m = 1, \ldots, \mu_b$, $\delta = n+1, \ldots, N$, $j = 1, \ldots, m_{b,\delta}$, $p = 1, \ldots, 4$.

A.1 Collocated element integrals

The collocated element integrals are denoted by ${}^{d,b}_{\beta}A^{e;k,q}_{\iota;j,p}$, where all the superscripts and the subscript ι have exactly the same meaning as for the coefficient tensor B. However, their default ranges are restricted to

$$
d = n+1, \ldots, N, \quad b = 0, \tfrac{1}{2}, 1, \quad e = 0, 1, \quad k = 1, \ldots, m_{b,d}, \quad q = 1, 2, 3
$$

with the proviso that the combination $k = 1$ and $q = 1$ is excluded. The cases $b = 0, 1$, $e = 1$ are also omitted, since they refer to the DtN conditions whose element integrals are denoted differently. The subscripts range by default as

$$
\beta = 0, \tfrac{1}{2}, 1, \tfrac{3}{2}, \quad \iota = 0, 1, \quad j = 1, \ldots, m_{\beta,d,e}, \quad p = 1, \ldots, 4,
$$

where

$$
m_{\beta,d,e} = \begin{cases} m_{\beta,d-e} & \text{for } \beta = 0, \frac{1}{2}, 1 \\ m_{\frac{1}{2},d+1-e} & \text{for } \beta = \frac{3}{2} \end{cases}
$$

Index β is a boundary label that combined with domain index d and equation label e identifies on which boundary the integration element is placed. The integers

j and p are integration element index and the index for the corresponding local basis functions, respectively. To simplify the notation for the element integrands, we abbreviate argument lists for the Green's functions and their derivatives. The original *vector* arguments consisting of field point and source point are replaced by two *scalar* arguments, where the first one denotes collocation point and the second one is the parameter for the integration path. An illustrating example is that

$$G_d({}^{d,0}x_1^{k,q}, t) \stackrel{\text{def}}{=} G_d(\boldsymbol{x}', \boldsymbol{x})$$

for field (collocation) point $\boldsymbol{x}' = ({}^{d,0}x_1^{k,q}, 0)$ and source point $\boldsymbol{x} = (x_1(t), x_2(t)) \in \Gamma_d$ parametrized by t. The auxiliary symbol ε_β is defined such that

$$\varepsilon_\beta = \begin{cases} -1 & \text{for } \beta = 0, \frac{1}{2} \\ \;\;1 & \text{for } \beta = 1, \frac{3}{2} \end{cases}$$

For axial symmetry, the evaluations of the restricted Green's function and its normal derivative (Section 2.2) involve the integration over the azimuthal source coordinate ϕ. The integrands concerned are periodic, from which it follows that G_d and $\frac{\partial G_d}{\partial n}$ do not depend on the azimuthal field coordinate ϕ'. By the reparametrization $\alpha = \frac{1}{2}(\phi - \phi')$ and by exploiting a symmetry of the integrands around $\alpha = \frac{\pi}{2}$, the angular integration is simplified into

$$\text{(31a)} \qquad G_d(\boldsymbol{x}', \boldsymbol{x}) = \frac{\kappa_d}{\pi} \int_0^{\frac{\pi}{2}} \xi^{-1} \exp(i\xi) d\alpha,$$

$$\text{(31b)} \qquad \frac{\partial G_d}{\partial n}(\boldsymbol{x}', \boldsymbol{x}) = \frac{\kappa_d}{\pi} \int_0^{\frac{\pi}{2}} (\xi^{-1} - i) \exp(i\xi) C_\beta(\boldsymbol{x}', \boldsymbol{x}, \alpha) d\alpha,$$

where

$$\xi = \kappa_d \left((x_1' - x_1)^2 + (x_2' - x_2)^2 + 4\eta(x_2')\eta(x_2) \sin^2(\alpha) \right)^{\frac{1}{2}},$$

$$C_\beta(\boldsymbol{x}', \boldsymbol{x}, \alpha) = \frac{\varepsilon_\beta}{\eta_t} \begin{cases} \dfrac{\left(x_1' - x_1(t)\right)\frac{dx_2}{dt} - \left(x_2' - x_2(t)\right)\frac{dx_1}{dt} + 2\eta(x_2')\frac{dx_1}{dt}\sin^2(\alpha)}{\left(x_1' - x_1(t)\right)^2 + \left(x_2' - x_2(t)\right)^2 + 4\eta(x_2')\eta(x_2(t))\sin^2(\alpha)}, & \boldsymbol{x}(t) \neq \boldsymbol{x}' \\ \dfrac{1}{2\eta(x_2(t))} \dfrac{dx_1}{dt}, & \boldsymbol{x}(t) = \boldsymbol{x}' \end{cases}$$

for $\beta = \frac{1}{2}$ with $\boldsymbol{x}(t) \in \Gamma_d$, and for $\beta = \frac{3}{2}$ with $\boldsymbol{x}(t) \in \Gamma_{d+1}$;

$$C_\beta(\boldsymbol{x}', \boldsymbol{x}, \alpha) = \varepsilon_\beta \begin{cases} \dfrac{x_2' - \beta r^1 - 2\eta(x_2')\sin^2(\alpha)}{(x_1' - x_1)^2 + (x_2' - \beta r^1)^2 + 4\eta(x_2')\eta(\beta r^1)\sin^2(\alpha)}, & x_1 \neq x_1' \\ -\dfrac{1}{2\eta(\beta r^1)}, & x_2' = \beta r^1,\ x_1 = x_1' \end{cases}$$

for $\beta = 0, 1$. At $\boldsymbol{x} = \boldsymbol{x}'$, $\alpha = 0$, the functions C_β have been defined by

$$C_\beta(\boldsymbol{x}', \boldsymbol{x}', 0) = \lim_{\alpha \to 0} C_\beta(\boldsymbol{x}', \boldsymbol{x}', \alpha) \neq \lim_{\boldsymbol{x} \to \boldsymbol{x}'} C_\beta(\boldsymbol{x}', \boldsymbol{x}, 0),$$

where the latter limits exist nota bene.

Index ranges that are omitted in formulas below are assumed to traverse their default values v.s. Evaluation of (17) and (18) at collocation points on the vertical boundaries yields the element integrals

$$\text{(32a)}\qquad {}^{d,b}_{\ \beta}A^{0;k,q}_{0;j,p} = \varepsilon_\beta \eta(\beta r^1) \int\limits_{{}^{d,\beta}x_1^{j-1}}^{{}^{d,\beta}x_1^{j}} \frac{\partial G_d}{\partial x_2}({}^{d,b}x_1^{k,q}, x_1)\varphi_{j,p}(x_1)dx_1,$$

$$\text{(32b)}\qquad {}^{d,b}_{\ \beta}A^{0;k,q}_{1;j,p} = -\eta(\beta r^1) \int\limits_{{}^{d,\beta}x_1^{j-1}}^{{}^{d,\beta}x_1^{j}} G_d({}^{d,b}x_1^{k,q}, x_1)\varphi_{j,p}(x_1)dx_1,$$

where $d = n+1,\dots,N$, $b = 0,1$, $\beta = 0,1$. For *plane symmetry*, the vertical boundaries are not curved leading to

$$ {}^{d,\underline{b}}_{\ b}A^{0;k,q}_{0;j,p} = 0, \quad \text{for } b = 0,1.$$

Evaluation of (15) at collocation points on the vertical boundaries yields the element integrals

$$ {}^{d,b}_{\ \beta}A^{0;k,q}_{0;j,p} = \varepsilon_\beta \int\limits_{{}^{d}t^{j-1}}^{{}^{d}t^{j}} \Big(\frac{\partial G_d}{\partial x_1}({}^{d,b}x_1^{k,q}, t)\frac{dx_2}{dt} - \frac{\partial G_d}{\partial x_2}({}^{d,b}x_1^{k,q}, t)\frac{dx_1}{dt}\Big)\eta\varphi_{j,p}(t)dt,$$

$$ {}^{d,b}_{\ \beta}A^{0;k,q}_{1;j,p} = \int\limits_{{}^{d}t^{j-1}}^{{}^{d}t^{j}} -G_d({}^{d,b}x_1^{k,q}, t)\eta\eta_t\varphi_{j,p}(t)dt,$$

where $d = n+1,\dots,N$, $b = 0,1$, $\beta = \frac{1}{2}$.

Evaluation of (16a) at collocation points on the vertical boundaries yields the element integrals

$$ {}^{d,b}_{\ \beta}A^{0;k,q}_{0;j,p} = \varepsilon_\beta \int\limits_{{}^{d+1}t^{j-1}}^{{}^{d+1}t^{j}} \Big(\frac{\partial G_d}{\partial x_1}({}^{d,b}x_1^{k,q}, t)\frac{dx_2}{dt} - \frac{\partial G_d}{\partial x_2}({}^{d,b}x_1^{k,q}, t)\frac{dx_1}{dt}\Big)\eta\varphi_{j,p}(t)dt,$$

$$ {}^{d,b}_{\ \beta}A^{0;k,q}_{1;j,p} = \frac{\varrho_d}{\varrho_{d+1}} \int\limits_{{}^{d+1}t^{j-1}}^{{}^{d+1}t^{j}} G_d({}^{d,b}x_1^{k,q}, t)\eta\eta_t\varphi_{j,p}(t)dt,$$

where $d = n+1,\dots,N-1$, $b = 0,1$, $\beta = \frac{3}{2}$.

The approximation (16b) results in

$$ {}^{N,b}_{\beta}A^{0;k,q}_{\iota;j,p} = 0, \quad \text{for } \beta = \tfrac{3}{2}. $$

Evaluation of (17) and (18) at collocation points on the interfaces yields the element integrals

$$ {}^{d,\frac{1}{2}}_{\beta}A^{e;k,q}_{0;j,p} = \varepsilon_\beta \eta(\beta r^1) \int\limits_{{}^{d-e,\beta}x_1^{j-1}}^{{}^{d-e,\beta}x_1^{j}} \frac{\partial G_{d-e}}{\partial x_2}({}^{d}t^{k,q}, x_1)\varphi_{j,p}(x_1)dx_1, $$

$$ {}^{d,\frac{1}{2}}_{\beta}A^{e;k,q}_{1;j,p} = -\eta(\beta r^1) \int\limits_{{}^{d-e,\beta}x_1^{j-1}}^{{}^{d-e,\beta}x_1^{j}} G_{d-e}({}^{d}t^{k,q}, x_1)\varphi_{j,p}(x_1)dx_1, $$

where $\beta = 0, 1$, $d = \begin{cases} n+1, \dots, N \text{ for } e = 0 \\ n+2, \dots, N \text{ for } e = 1 \end{cases}$

Evaluation of (15) at collocation points on the interfaces yields the element integrals

$$ \text{(33a)} \quad {}^{d,\frac{1}{2}}_{\beta}A^{e;k,q}_{0;j,p} = \varepsilon_\beta \int\limits_{{}^{d-e}t^{j-1}}^{{}^{d-e}t^{j}} \Big(\frac{\partial G_{d-e}}{\partial x_1}({}^{d}t^{k,q}, t)\frac{dx_2}{dt} - \frac{\partial G_{d-e}}{\partial x_2}({}^{d}t^{k,q}, t)\frac{dx_1}{dt}\Big)\eta\varphi_{j,p}(t)dt, $$

$$ \text{(33b)} \quad {}^{d,\frac{1}{2}}_{\beta}A^{e;k,q}_{1;j,p} = \int\limits_{{}^{d-e}t^{j-1}}^{{}^{d-e}t^{j}} -G_{d-e}({}^{d}t^{k,q}, t)\eta\eta_t\varphi_{j,p}(t)dt, $$

where $\beta = \frac{1}{2}$, $d = \begin{cases} n+1, \dots, N \text{ for } e = 0 \\ n+2, \dots, N \text{ for } e = 1 \end{cases}$

Evaluation of (16a) at collocation points on the interfaces yields the element integrals

$$ \text{(34a)} \quad {}^{d,\frac{1}{2}}_{\beta}A^{e;k,q}_{0;j,p} = \varepsilon_\beta \int\limits_{{}^{d+1-e}t^{j-1}}^{{}^{d+1-e}t^{j}} \Big(\frac{\partial G_{d-e}}{\partial x_1}({}^{d}t^{k,q}, t)\frac{dx_2}{dt} - \frac{\partial G_{d-e}}{\partial x_2}({}^{d}t^{k,q}, t)\frac{dx_1}{dt}\Big)\eta\varphi_{j,p}(t)dt, $$

$$ \text{(34b)} \quad {}^{d,\frac{1}{2}}_{\beta}A^{e;k,q}_{1;j,p} = \frac{\varrho_{d-e}}{\varrho_{d+1-e}} \int\limits_{{}^{d+1-e}t^{j-1}}^{{}^{d+1-e}t^{j}} G_{d-e}({}^{d}t^{k,q}, t)\eta\eta_t\varphi_{j,p}(t)dt, $$

where $\beta = \frac{3}{2}$, $d = \begin{cases} n+1, \dots, N-1 & \text{for } e = 0 \\ n+2, \dots, N & \text{for } e = 1 \end{cases}$

Since BIE (22) is not valid for $d = n + 1$, the components ${}^{n+1,\frac{1}{2}}_{\beta}A^{1;k,q}_{\iota;j,p}$ are redundant.

A.2 Quadrature

The polynomial degree of the approximants is chosen to yield a numerical solution that is (normwise) fourth-order accurate w.r.t. the (maximal) element length. In order to prevent the numerical integration from contributing significantly to the truncation error, it is appropriate that the quadrature rules have a global order of accuracy at least 5. To raise it above 6 is futile, since the computational cost would rise without any virtual decrease of the total error. From a numerical perspective, three types of collocated element integrals arise. The crucial point is that for an element integral where the collocation point belongs to the element, the integrand exhibits an integrable singularity.

A.2.1 Regular and quasisingular integrands

For those element integrals where the smallest distance from such an integral's collocation point to its element is sufficiently large, the integrands are regular (in the sense that they are well approximated by low degree polynomials). By employing three-point Gauss–Legendre quadrature, the element integrals with regular integrands are computed adequately accurate (v.s.). We advocate that the integrations in (31) should be done approximately with the trapezoidal rule, since it is surprisingly accurate [5, Sec. 2.9] for such semiperiodic cases.

For an element integral where the smallest distance from the collocation point to the element is less than some fraction ($\tau \approx 10\%$) of a wavelength, the integrand is called quasisingular [7, p. 176]. The distinction between regular and quasisingular integrands is inherently fuzzy, i.e., the value of the tolerance τ is a choice. For quasisingular integrands, there is a risk that common integration methods (such as Gauss–Legendre quadrature) may be insufficiently accurate. Even though the integrand is nonsingular and the quadrature rule has an adequate order of accuracy, the proximity to the singularity could render the remainder term (typically containing a high derivative of the integrand) too large. The remedy is to use some adaptive quadrature tailored for the given singularity. An ad hoc handling of the quasisingular case is to exploit the regular quadrature rule mentioned above (three-point Gauss–Legendre) in its *composite* form on a (possibly nonuniform) division of the element concerned into a moderate number (< 10) of subintervals.

A.2.2 Singular integrands along the interfaces

For element integrals where the collocation points belong to the elements, the integrands exhibit integrable singularities at those collocation points. Common quadrature formulas cannot be expected to be sufficiently accurate, even when the quadrature abscissas are separated from the singular points. Special integration techniques adapted to the singularites are required. Along the interfaces such singularities are found by considering the integrals (33) for $\beta = \frac{1}{2}$, $e = 0$, and (34) for $\beta = \frac{3}{2}$, $e = 1$, where indices d, k, and p traverse their default values. The formulas could be combined into

$$
{}^{d,\frac{1}{2}}_{\beta}A^{e;k,q}_{0;j,p} = \varepsilon_\beta \int\limits_{{}^d t^{j-1}}^{{}^d t^{j}} \Big(\frac{\partial G_{d-e}}{\partial x_1}({}^d t^{k,q}, t)\frac{dx_2}{dt} - \frac{\partial G_{d-e}}{\partial x_2}({}^d t^{k,q}, t)\frac{dx_1}{dt}\Big)\eta\varphi_{j,p}(t)dt,
$$

$$
{}^{d,\frac{1}{2}}_{\beta}A^{e;k,q}_{1;j,p} = \varepsilon_\beta \frac{\varrho_{d-e}}{\varrho_d} \int\limits_{{}^d t^{j-1}}^{{}^d t^{j}} G_{d-e}({}^d t^{k,q}, t)\eta\eta_t\varphi_{j,p}(t)dt,
$$

where the singular cases are given by $j = k$, $q = 2, 3$, and $j = k-1, k$, $q = 1$. For the case $j = k$ and $q = 2, 3$, the integrals over $[{}^d t^{j-1}, {}^d t^{j}]$ are divided into sums of integrals over $[{}^d t^{k-1}, {}^d t^{k,q})$ and $({}^d t^{k,q}, {}^d t^{k}]$ in order to get the singular point $t = {}^d t^{k,q}$ as an endpoint.

A.2.2.I

For the subintegrals over $({}^d t^{k,q}, {}^d t^{k}]$, use the parametrization $0 < \sigma \leq 1$ such that $t = {}^d t^{k,q} + \frac{4-q}{3} h^k_d \sigma$. By the decomposition techniques described below, the contributions from $({}^d t^{k,q}, {}^d t^{k}]$ are expressed as

$$
\int\limits_{{}^d t^{k,q}}^{{}^d t^{k}} \Big(\frac{\partial G_{d-e}}{\partial x_1}({}^d t^{k,q}, t)\frac{dx_2}{dt} - \frac{\partial G_{d-e}}{\partial x_2}({}^d t^{k,q}, t)\frac{dx_1}{dt}\Big)\eta\varphi_{k,p}(t)dt = \tfrac{4-q}{3} h^k_d (S_0 + R_0),
$$

$$
\int\limits_{{}^d t^{k,q}}^{{}^d t^{k}} G_{d-e}({}^d t^{k,q}, t)\eta\eta_t\varphi_{k,p}(t)dt = \tfrac{4-q}{3} h^k_d (S_1 + R_1),
$$

which is referred to as Case 2.I.

Plane symmetry

For plane symmetry, the Green's function and its normal derivative are split into terms containing the logarithmic singularity as a factor and regular remainder terms. This leads to decompositions into integrals R_ι with regular integrands and integrals S_ι, $\iota = 1, 0$, where the integrand is a product of a logarithm and a smooth function. To this end, introduce the auxiliary quantities

$$
\begin{aligned}
\xi &= \kappa_{d-e}\left((x_1({}^dt^{k,q}) - x_1(t))^2 + (x_2({}^dt^{k,q}) - x_2(t))^2\right)^{\frac{1}{2}},\\
D(t) &= \kappa_{d-e}^2\left((x_1({}^dt^{k,q}) - x_1(t))\tfrac{dx_2}{dt} - (x_2({}^dt^{k,q}) - x_2(t))\tfrac{dx_1}{dt}\right),\\
C(t) &= \begin{cases} \dfrac{\big(x_1({}^dt^{k,q}) - x_1(t)\big)\frac{dx_2}{dt} - \big(x_2({}^dt^{k,q}) - x_2(t)\big)\frac{dx_1}{dt}}{\big(x_1({}^dt^{k,q}) - x_1(t)\big)^2 + \big(x_2({}^dt^{k,q}) - x_2(t)\big)^2}, & t \neq {}^dt^{k,q}\\ \dfrac{\eta_t^{-2}}{2}\Big(\dfrac{dx_2}{dt}\dfrac{d^2x_1}{dt^2} - \dfrac{dx_1}{dt}\dfrac{d^2x_2}{dt^2}\Big), & t = {}^dt^{k,q} \end{cases}
\end{aligned}
$$

Towards the extraction of the singularities at $\xi = 0$, appropriate truncations of the zeroth and first order Neumann functions for small arguments are

$$
\begin{aligned}
\mathrm{Y}_0(\xi) &\approx \frac{2}{\pi}\big(\ln(\xi) - \ln(2) + \gamma\big)\mathrm{J}_0(\xi) + \frac{1}{2\pi}\big(\xi^2 - \tfrac{3}{32}\xi^4 + \tfrac{11}{3456}\xi^6 - \tfrac{25}{442368}\xi^8\big),\\
\mathrm{Y}_1(\xi) &\approx -\frac{2}{\pi}\xi^{-1} + \frac{2}{\pi}\big(\ln(\xi) - \ln(2) + \gamma\big)\mathrm{J}_1(\xi) - \frac{1}{2\pi}\big(\xi - \tfrac{5}{16}\xi^3 + \tfrac{5}{288}\xi^5 - \tfrac{47}{110592}\xi^7\big),
\end{aligned}
$$

where γ is Euler's constant. By using these approximations and the scaling "trick" $\ln(\xi) = \ln(\sigma) + \ln(\xi) - \ln(\sigma) = \ln(\sigma) + \ln(\xi/\sigma)$, one obtains

$$
G_{d-e}({}^dt^{k,q}, t)\eta\eta_t = \frac{i}{4}\mathrm{H}_0^{(1)}(\xi)\eta_t = -\frac{1}{2\pi}\ln(\sigma)\mathrm{J}_0(\xi)\eta_t + \frac{1}{2\pi}g_0(\sigma),
$$

where

$$
g_0(\sigma) \approx \big(-\ln\big(\frac{\xi}{\sigma}\big) + \ln(2) - \gamma + i\frac{\pi}{2}\big)\mathrm{J}_0(\xi)\eta_t - \big(\tfrac{1}{4}\xi^2 - \tfrac{3}{128}\xi^4 + \tfrac{11}{13824}\xi^6 - \tfrac{25}{1769472}\xi^8\big)\eta_t,
$$

and

$$
\begin{aligned}
\Big(\frac{\partial G_{d-e}}{\partial x_1}({}^dt^{k,q}, t)\frac{dx_2}{dt} - \frac{\partial G_{d-e}}{\partial x_2}({}^dt^{k,q}, t)\frac{dx_1}{dt}\Big)\eta &= \frac{i}{4}\frac{\mathrm{H}_1^{(1)}(\xi)}{\xi}D(t)\\
&= -\frac{1}{4\pi}\ln(\sigma)\big(\mathrm{J}_0(\xi) + \mathrm{J}_2(\xi)\big)D(t) + \frac{1}{4\pi}g_1(\sigma),
\end{aligned}
$$

where

$$
\begin{aligned}
g_1(\sigma) \approx 2C(t) &+ \big(-\ln\big(\frac{\xi}{\sigma}\big) + \ln(2) - \gamma + i\frac{\pi}{2}\big)\big(\mathrm{J}_0(\xi) + \mathrm{J}_2(\xi)\big)D(t)\\
&+ \big(\tfrac{1}{2} - \tfrac{5}{32}\xi^2 + \tfrac{5}{576}\xi^4 - \tfrac{47}{221184}\xi^6\big)D(t).
\end{aligned}
$$

The remainder functions $g_0(\sigma)$ and $g_1(\sigma)$ are smooth and bounded, even in the limit $\sigma \to 0$.

For $j = k$ and $q = 2, 3$, the integrals in Case 2.i are now identified by

(35a) $$S_1 = \frac{1}{2\pi}\int_0^1 -\ln(\sigma)\,\mathrm{J}_0(\xi)\eta_t\,\varphi_{j,p}(s)d\sigma,$$

(35b) $$S_0 = \frac{1}{4\pi}\int_0^1 -\ln(\sigma)\,\big(\mathrm{J}_0(\xi) + \mathrm{J}_2(\xi)\big)D(t)\,\varphi_{j,p}(s)d\sigma,$$

and

(36a) $$R_1 = \frac{1}{2\pi} \int_0^1 g_0(\sigma) \varphi_{j,p}(s) d\sigma,$$

(36b) $$R_0 = \frac{1}{4\pi} \int_0^1 g_1(\sigma) \varphi_{j,p}(s) d\sigma,$$

where

$$t = {}^{d}t^{k,q} + \tfrac{4-q}{3} h_d^k \sigma,$$
$$s = \tfrac{2}{3}(4-q)(\sigma - 1) + 1.$$

Following the principles in Section A.2.1, an adequate way of computing integrals (35) is to employ logarithmically weighted Gaussian quadrature [21, Tab. 9] with three points. Integrals (36) are treated as the regular case, i.e., by using three-point Gauss–Legendre quadrature.

Axial symmetry

For axial symmetry, the angular integration in (31) renders the integrals in Case 2.I two-dimensional. The singularities at the point $t = {}^{d}t^{k,q}$ $(\sigma = 0)$, $\alpha = 0$ can be removed by a regularizing transformation due to Lachat and Watson [11]. The principle is to divide the rectangular integration element (on which the integrand has a corner singularity) into two triangles for which the integrands have reciprocal edge singularities. The latter singularities are cancelled out by zeros for the Jacobian determinant of the Lachat–Watson transformation.

The original integration strip $0 < \sigma \leq 1$, $0 < \alpha \leq \frac{\pi}{2}$ is divided along a diagonal into the two triangles

$$0 < \sigma \leq 1, \quad 0 < \alpha \leq \sigma \tfrac{\pi}{2},$$
$$0 < \alpha \leq \tfrac{\pi}{2}, \quad 0 < \sigma \leq \alpha \tfrac{2}{\pi}.$$

Under the substitution $\alpha = \sigma\widetilde{\alpha}$ or $\sigma = \alpha\widetilde{\sigma}$ of either integration variable, the triangles obtain the parametrizations

$$0 < \sigma \leq 1, \quad 0 < \widetilde{\alpha} \leq \tfrac{\pi}{2},$$
$$0 < \alpha \leq \tfrac{\pi}{2}, \quad 0 < \widetilde{\sigma} \leq \tfrac{2}{\pi},$$

and the differential $d\alpha d\sigma$ is transformed into $\sigma d\widetilde{\alpha} d\sigma$ or $\alpha d\alpha d\widetilde{\sigma}$. For domain index $d - e$ and collocation point $\boldsymbol{x}' = \boldsymbol{x}({}^{d}t^{k,q})$, the singular factor ξ^{-1} arising in (31) is factorized (dropping the $\widetilde{\ }$ for notational convenience) as

$$\xi^{-1} = \begin{cases} \sigma^{-1} \xi_\sigma^{-1} & \text{for } \alpha \mapsto \sigma\alpha \\ \alpha^{-1} \xi_\alpha^{-1} & \text{for } \sigma \mapsto \alpha\sigma \end{cases}$$

where

$$\xi_\sigma = \kappa_{d-e}\Big(\big(\tfrac{x_1({}^dt^{k,q})-x_1(t)}{\sigma}\big)^2 + \big(\tfrac{x_2({}^dt^{k,q})-x_2(t)}{\sigma}\big)^2 + 4\eta\big(x_2({}^dt^{k,q})\big)\eta\big(x_2(t)\big)\alpha^2\mathrm{sinc}^2(\sigma\alpha)\Big)^{\frac{1}{2}},$$
$$\xi_\alpha = \kappa_{d-e}\Big(\big(\tfrac{x_1({}^dt^{k,q})-x_1(t)}{\alpha}\big)^2 + \big(\tfrac{x_2({}^dt^{k,q})-x_2(t)}{\alpha}\big)^2 + 4\eta\big(x_2({}^dt^{k,q})\big)\eta\big(x_2(t)\big)\mathrm{sinc}^2(\alpha)\Big)^{\frac{1}{2}},$$

where sinc denotes the *unnormalized* cardinal sine function. The formula

$$\xi^{-1}d\alpha d\sigma = \begin{cases} \sigma^{-1}\xi_\sigma^{-1}\sigma d\widetilde{\alpha}d\sigma = \xi_\sigma^{-1}d\widetilde{\alpha}d\sigma \\ \alpha^{-1}\xi_\alpha^{-1}\alpha d\alpha d\widetilde{\sigma} = \xi_\alpha^{-1}d\alpha d\widetilde{\sigma} \end{cases}$$

shows that the singularities are removable, since ξ_σ^{-1} and ξ_α^{-1} are bounded particularly in the limits $\sigma \to 0$ and $\alpha \to 0$. The decompositions in Case 2.I are achieved by performing the Lachat–Watson transformation, where the integrals S_ι and R_ι, $\iota = 1, 0$, correspond to the substitutions $\alpha \mapsto \sigma\alpha$ and $\sigma \mapsto \alpha\sigma$, respectively. The function

$$C(t,\alpha) = \begin{cases} \frac{\big(x_1({}^dt^{k,q})-x_1(t)\big)\frac{dx_2}{dt}-\big(x_2({}^dt^{k,q})-x_2(t)\big)\frac{dx_1}{dt}+2\eta(x_2({}^dt^{k,q}))\frac{dx_1}{dt}\sin^2(\alpha)}{\big(x_1({}^dt^{k,q})-x_1(t)\big)^2+\big(x_2({}^dt^{k,q})-x_2(t)\big)^2+4\eta(x_2({}^dt^{k,q}))\eta(x_2(t))\sin^2(\alpha)}\eta(x_2(t)), & t \neq {}^dt^{k,q} \\ \frac{1}{2}\frac{dx_1}{dt}, & t = {}^dt^{k,q} \end{cases}$$

is introduced in order to abbreviate the expression

$$C_\beta(\boldsymbol{x}({}^dt^{k,q}), \boldsymbol{x}(t), \alpha)\eta(x_2(t))\eta_t \equiv \varepsilon_\beta C(t,\alpha), \quad \beta = \tfrac{1}{2}, \tfrac{3}{2}$$

originating from (31).

For $j = k$ and $q = 2, 3$, the integrals in Case 2.I become

$$S_1 = \frac{\kappa_{d-e}}{\pi}\int_0^1\int_0^{\frac{\pi}{2}} \xi_\sigma^{-1}\exp(i\sigma\xi_\sigma)d\alpha\,\eta\eta_t\,\varphi_{j,p}(s)d\sigma, \tag{37a}$$

$$S_0 = \frac{\kappa_{d-e}}{\pi}\int_0^1\int_0^{\frac{\pi}{2}} (\xi_\sigma^{-1} - i\sigma)\exp(i\sigma\xi_\sigma)C(t,\sigma\alpha)d\alpha\,\varphi_{j,p}(s)d\sigma, \tag{37b}$$

where

$$t = {}^dt^{k,q} + \tfrac{4-q}{3}h_d^k\sigma,$$
$$s = \tfrac{2}{3}(4-q)(\sigma-1)+1,$$

and

$$R_1 = \frac{\kappa_{d-e}}{\pi}\int_0^{\frac{2}{\pi}}\int_0^{\frac{\pi}{2}} \xi_\alpha^{-1}\exp(i\alpha\xi_\alpha)\eta\eta_t\,\varphi_{j,p}(s)d\alpha d\sigma, \tag{38a}$$

$$R_0 = \frac{\kappa_{d-e}}{\pi}\int_0^{\frac{2}{\pi}}\int_0^{\frac{\pi}{2}} (\xi_\alpha^{-1} - i\alpha)\exp(i\alpha\xi_\alpha)C(t,\alpha)\,\varphi_{j,p}(s)d\alpha d\sigma, \tag{38b}$$

where

$$t = {}^{d}t^{k,q} + \tfrac{4-q}{3} h_d^k \sigma\alpha,$$
$$s = \tfrac{2}{3}(4-q)(\sigma\alpha - 1) + 1.$$

Even though the integrands to S_ι and R_ι are nonsingular, the quadrature formulas must be designed carefully, since the integrands to S_ι typically are stiff for $\alpha \approx 0$.

A.2.2.II

The contributions from $[\,{}^{d}t^{k-1}, {}^{d}t^{k,q})$ are decomposed as

$$\int_{{}^{d}t^{k-1}}^{{}^{d}t^{k,q}} \Big(\frac{\partial G_{d-e}}{\partial x_1}({}^{d}t^{k,q}, t)\frac{dx_2}{dt} - \frac{\partial G_{d-e}}{\partial x_2}({}^{d}t^{k,q}, t)\frac{dx_1}{dt}\Big)\eta\varphi_{k,p}(t)dt = \tfrac{q-1}{3} h_d^k (S_0 + R_0),$$

$$\int_{{}^{d}t^{k-1}}^{{}^{d}t^{k,q}} G_{d-e}({}^{d}t^{k,q}, t)\eta\eta_t\varphi_{k,p}(t)dt = \tfrac{q-1}{3} h_d^k (S_1 + R_1),$$

which is referred to as Case 2.II.

Plane symmetry

For $j = k$ and $q = 2, 3$, the integrals in Case 2.II obey formulas (35) and (36) *with*

$$t = {}^{d}t^{k,q} - \tfrac{q-1}{3} h_d^k \sigma,$$
$$s = \tfrac{2}{3}(q-1)(1-\sigma) - 1.$$

Axial symmetry

For $j = k$ and $q = 2, 3$, the integrals S_ι in Case 2.II obey formulas (37) *with*

$$t = {}^{d}t^{k,q} - \tfrac{q-1}{3} h_d^k \sigma,$$
$$s = \tfrac{2}{3}(q-1)(1-\sigma) - 1,$$

and the corresponding R_ι obey formulas (38) *with*

$$t = {}^{d}t^{k,q} - \tfrac{q-1}{3} h_d^k \sigma\alpha,$$
$$s = \tfrac{2}{3}(q-1)(1-\sigma\alpha) - 1.$$

A.2.2.III

For the case $j = k-1, k$ and $q = 1$, the singular point $t = {}^{d}t^{k,1}$ coincides with the integration endpoint ${}^{d}t^{k-1}$ resulting in the decompositions

$$\int_{{}^{d}t^{j-1}}^{{}^{d}t^{j}} \Big(\frac{\partial G_{d-e}}{\partial x_1}({}^{d}t^{k,1}, t)\frac{dx_2}{dt} - \frac{\partial G_{d-e}}{\partial x_2}({}^{d}t^{k,1}, t)\frac{dx_1}{dt} \Big) \eta\varphi_{j,p}(t)dt = h_d^j(S_0 + R_0),$$

$$\int_{{}^{d}t^{j-1}}^{{}^{d}t^{j}} G_{d-e}({}^{d}t^{k,1}, t)\eta\eta_t\varphi_{j,p}(t)dt = h_d^j(S_1 + R_1),$$

which is referred to as Case 2.III.

Plane symmetry

For $j = k-1$ and $q = 1$, the integrals in Case 2.III obey formulas (35) and (36) *with*

$$t = {}^{d}t^{k,1} - h_d^{k-1}\sigma,$$
$$s = 2(1-\sigma) - 1.$$

For $j = k$ and $q = 1$, the integrals in Case 2.III obey formulas (35) and (36).

Axial symmetry

For $j = k-1$ and $q = 1$, the integrals S_ι in Case 2.III obey formulas (37) *with*

$$t = {}^{d}t^{k,1} - h_d^{k-1}\sigma,$$
$$s = 2(1-\sigma) - 1,$$

and the corresponding R_ι obey formulas (38) *with*

$$t = {}^{d}t^{k,1} - h_d^{k-1}\sigma\alpha,$$
$$s = 2(1-\sigma\alpha) - 1.$$

For $j = k$ and $q = 1$, the integrals in Case 2.III obey formulas (37) and (38).

A.2.3 Singular integrands along the vertical boundaries

The previously described technique to handle singular integrands along the interfaces is applicable also for the vertical boundaries. This section contains a brief presentation of the latter case. Consider the integrals (32) for $\beta = b = 0, 1$, yielding

$$
{}^{d,\underline{b}}_{\;b}A^{0;k,q}_{0;j,p} = \varepsilon_b \eta(br^1) \int_{{}^{d,b}x_1^{j-1}}^{{}^{d,b}x_1^{j}} \frac{\partial G_d}{\partial x_2}({}^{d,b}x_1^{k,q}, x_1)\varphi_{j,p}(x_1)dx_1,
$$

$$
{}^{d,\underline{b}}_{\;b}A^{0;k,q}_{1;j,p} = -\eta(br^1) \int_{{}^{d,b}x_1^{j-1}}^{{}^{d,b}x_1^{j}} G_d({}^{d,b}x_1^{k,q}, x_1)\varphi_{j,p}(x_1)dx_1,
$$

where the singular cases are given by $j = k$, $q = 2, 3$, and $j = k-1, k$, $q = 1$. For the case $j = k$ and $q = 2, 3$, the integration interval $[{}^{d,b}x_1^{j-1}, {}^{d,b}x_1^{j}]$ is divided into $[{}^{d,b}x_1^{k-1}, {}^{d,b}x_1^{k,q})$ and $({}^{d,b}x_1^{k,q}, {}^{d,b}x_1^{k}]$.

A.2.3.I

For the subintegrals over $({}^{d,b}x_1^{k,q}, {}^{d,b}x_1^{k}]$, use the parametrization $0 < \sigma \leq 1$ such that $x_1 = {}^{d,b}x_1^{k,q} + \frac{4-q}{3}h_{b,d}\sigma$. The contributions from $({}^{d,b}x_1^{k,q}, {}^{d,b}x_1^{k}]$ are decomposed as

$$
\int_{{}^{d,b}x_1^{k,q}}^{{}^{d,b}x_1^{k}} \eta(br^1)\frac{\partial G_d}{\partial x_2}({}^{d,b}x_1^{k,q}, x_1)\varphi_{k,p}(x_1)dx_1 = \tfrac{4-q}{3}h_{b,d}(S_0 + R_0),
$$

$$
\int_{{}^{d,b}x_1^{k,q}}^{{}^{d,b}x_1^{k}} \eta(br^1)G_d({}^{d,b}x_1^{k,q}, x_1)\varphi_{k,p}(x_1)dx_1 = \tfrac{4-q}{3}h_{b,d}(S_1 + R_1),
$$

which is referred to as Case 3.I.

Plane symmetry

For $j = k$ and $q = 2, 3$, the nontrivial integrals in Case 3.I become

$$
S_1 = \frac{1}{2\pi}\int_0^1 -\ln(\sigma)\,\mathrm{J}_0(\xi)\,\varphi_{j,p}(s)d\sigma, \tag{39a}
$$

$$
R_1 = \frac{1}{2\pi}\int_0^1 g_0(\sigma)\varphi_{j,p}(s)d\sigma, \tag{39b}
$$

where

(39c) $$g_0(\sigma) \approx \big(-\ln(\tfrac{4-q}{3}\kappa_d h_{b,d}) + \ln(2) - \gamma + i\frac{\pi}{2}\big)\mathrm{J}_0(\xi) - (\tfrac{1}{4}\xi^2 - \tfrac{3}{128}\xi^4 + \tfrac{11}{13824}\xi^6 - \tfrac{25}{1769472}\xi^8),$$

(39d) $$\xi = \tfrac{4-q}{3}\kappa_d h_{b,d}\sigma,$$
$$s = \tfrac{2}{3}(4-q)(\sigma-1)+1.$$

Axial symmetry

The function

$$C_b(\sigma,\alpha) = \begin{cases} \dfrac{-2\eta^2(br^1)\sin^2(\alpha)}{h_{b,d}^2\sigma^2 + 4\eta^2(br^1)\sin^2(\alpha)}, & \sigma \neq 0 \\ -\frac{1}{2}, & \sigma = 0 \end{cases}$$

is introduced in order to abbreviate the expression

$$C_b(\boldsymbol{x}', \boldsymbol{x}, \alpha)\eta(br^1) \equiv \varepsilon_b C_b(\tfrac{4-q}{3}\sigma, \alpha), \quad b = 0, 1$$

for

$$\boldsymbol{x}' = ({}^{d,b}x_1^{k,q}, br^1),$$
$$\boldsymbol{x} = ({}^{d,b}x_1^{k,q} + \tfrac{4-q}{3}h_{b,d}\sigma, br^1).$$

For $j = k$ and $q = 2, 3$, the integrals in Case 3.I become

(40a) $$S_1 = \eta(br^1)\frac{\kappa_d}{\pi}\int_0^1\int_0^{\frac{\pi}{2}} \xi^{-1}\exp(i\sigma\xi)d\alpha\, \varphi_{j,p}(s)d\sigma,$$

(40b) $$S_0 = \frac{\kappa_d}{\pi}\int_0^1\int_0^{\frac{\pi}{2}} (\xi^{-1} - i\sigma)\exp(i\sigma\xi)C_b(\tfrac{4-q}{3}\sigma, \sigma\alpha)d\alpha\, \varphi_{j,p}(s)d\sigma,$$

where

(40c) $$\xi = \kappa_d\left((\tfrac{4-q}{3})^2 h_{b,d}^2 + 4\eta^2(br^1)\alpha^2\mathrm{sinc}^2(\sigma\alpha)\right)^{\frac{1}{2}},$$
$$s = \tfrac{2}{3}(4-q)(\sigma-1)+1,$$

and

(41a) $$R_1 = \eta(br^1)\frac{\kappa_d}{\pi}\int_0^{\frac{2}{\pi}}\int_0^{\frac{\pi}{2}} \xi^{-1}\exp(i\alpha\xi)\,\varphi_{j,p}(s)d\alpha d\sigma,$$

(41b) $$R_0 = \frac{\kappa_d}{\pi}\int_0^{\frac{2}{\pi}}\int_0^{\frac{\pi}{2}} (\xi^{-1} - i\alpha)\exp(i\alpha\xi)C_b(\tfrac{4-q}{3}\sigma\alpha, \alpha)\,\varphi_{j,p}(s)d\alpha d\sigma,$$

where

$$\xi = \kappa_d \left((\tfrac{4-q}{3})^2 h_{b,d}^2 \sigma^2 + 4\eta^2(br^1)\operatorname{sinc}^2(\alpha) \right)^{\frac{1}{2}}, \tag{41c}$$
$$s = \tfrac{2}{3}(4-q)(\sigma\alpha - 1) + 1.$$

A.2.3.II

The contributions from $[\,{}^{d,b}x_1^{k-1},\ {}^{d,b}x_1^{k,q})$ are decomposed as

$$\int_{{}^{d,b}x_1^{k-1}}^{{}^{d,b}x_1^{k,q}} \eta(br^1)\frac{\partial G_d}{\partial x_2}(\,{}^{d,b}x_1^{k,q}, x_1)\varphi_{k,p}(x_1)dx_1 = \tfrac{q-1}{3}h_{b,d}(S_0 + R_0),$$
$$\int_{{}^{d,b}x_1^{k-1}}^{{}^{d,b}x_1^{k,q}} \eta(br^1)G_d(\,{}^{d,b}x_1^{k,q}, x_1)\varphi_{k,p}(x_1)dx_1 = \tfrac{q-1}{3}h_{b,d}(S_1 + R_1),$$

which is referred to as Case 3.II.

Plane symmetry

For $j = k$ and $q = 2, 3$, and under the proviso that $\frac{4-q}{3}$ is replaced by $\frac{q-1}{3}$, the nontrivial integrals in Case 3.II obey formulas (39) *with*

$$s = \tfrac{2}{3}(q-1)(1-\sigma) - 1.$$

Axial symmetry

For $j = k$ and $q = 2, 3$, and under the proviso that $\frac{4-q}{3}$ is replaced by $\frac{q-1}{3}$, the integrals S_ι in Case 3.II obey formulas (40) *with*

$$s = \tfrac{2}{3}(q-1)(1-\sigma) - 1,$$

and the corresponding R_ι obey formulas (41) *with*

$$s = \tfrac{2}{3}(q-1)(1-\sigma\alpha) - 1.$$

A.2.3.III

For the case $j = k-1, k$ and $q = 1$, the decompositions are

$$\int_{{}^{d,b}x_1^{j-1}}^{{}^{d,b}x_1^{j}} \eta(br^1)\frac{\partial G_d}{\partial x_2}(\,{}^{d,b}x_1^{k,1}, x_1)\varphi_{j,p}(x_1)dx_1 = h_{b,d}(S_0 + R_0),$$
$$\int_{{}^{d,b}x_1^{j-1}}^{{}^{d,b}x_1^{j}} \eta(br^1)G_d(\,{}^{d,b}x_1^{k,1}, x_1)\varphi_{j,p}(x_1)dx_1 = h_{b,d}(S_1 + R_1),$$

which is referred to as Case 3.III.

Plane symmetry

For $j = k - 1$ and $q = 1$, the nontrivial integrals in Case 3.III obey formulas (39) *with*

$$s = 2(1 - \sigma) - 1.$$

For $j = k$ and $q = 1$, the nontrivial integrals in Case 3.III obey formulas (39).

Axial symmetry

For $j = k - 1$ and $q = 1$, the integrals S_ι in Case 3.III obey formulas (40) *with*

$$s = 2(1 - \sigma) - 1,$$

and the corresponding R_ι obey formulas (41) *with*

$$s = 2(1 - \sigma\alpha) - 1.$$

For $j = k$ and $q = 1$, the integrals in Case 3.III obey formulas (40) and (41).

B Appendix

In order to facilitate the assembly of those components of B involving the DtN conditions for the top n layers, we introduce an auxiliary tensor with components ${}_{\delta,\beta}U^{e;k,q}_{0;j,p}$. For the case $e = 1$, the components of U are weights arising from finite difference approximations of $\frac{\partial p}{\partial n}(x_1, x_2)$ at the vertical boundaries $x_2 = 0$ and $x_2 = r^1$. The approximations are denoted by

$$-\frac{\partial p}{\partial x_2}(z^0_\delta, 0) \approx {}_{\underline{\delta},\frac{1}{2}}U^{1;1,1}_{0;1,p}\ {}^{\delta,\frac{1}{2}}v^{0;1,p},$$
$$\frac{\partial p}{\partial x_2}(z^1_\delta, r^1) \approx {}_{\underline{\delta},\frac{1}{2}}U^{1;1,m_2}_{0;1,p}\ {}^{\delta,\frac{1}{2}}v^{0;1,p},$$

and

$$-\frac{\partial p}{\partial x_2}({}^{\delta,0}x^k_1, 0) \approx {}_{\underline{\delta},1}U^{1;k,1}_{0;j,p}\ {}^{\delta,1}v^{0;j,p},$$
$$\frac{\partial p}{\partial x_2}({}^{\delta,1}x^k_1, r^1) \approx {}_{\underline{\delta},1}U^{1;k,m_2}_{0;j,p}\ {}^{\delta,1}v^{0;j,p},$$

for $\delta = 1, \ldots, n$, $k = 1, \ldots, m_{1,\delta}$, with the understanding that

$${}^{\delta,1}v^{0;0,p} \equiv {}^{\delta,\frac{1}{2}}v^{0;1,p},$$
$${}^{\delta,1}v^{0;m_{1,\delta}+1,p} \equiv {}^{\delta+1,\frac{1}{2}}v^{0;1,p}, \quad \delta = 1, \ldots, n-1,$$

and under the technical substitutions

$${}^{n,1}v^{0;j,1} \mapsto {}^{n+1,0}v^{1;0,1}, \quad {}^{n,1}v^{0;j,2} \mapsto {}^{n+1,0}v^{0;0,1},$$
$${}^{n,1}v^{0;j,m_2-1} \mapsto {}^{n+1,1}v^{0;0,1}, \quad {}^{n,1}v^{0;j,m_2} \mapsto {}^{n+1,1}v^{1;0,1},$$
$$j = m_{1,n} + 1.$$

On the interfaces ($\beta = \frac{1}{2}$), standard fourth-order accurate finite difference formulas are used, whereas a Numerov technique [4, pp. 167, 384] is employed for internal ($\beta = 1$) nodes. The resulting nonzero components with superscript $e = 1$ become

$${}_{\delta,\frac{1}{2}}U^{1;1,1}_{0;1,1} = \tfrac{11}{12}h^{-1}_{2,\delta}$$
$${}_{\delta,\frac{1}{2}}U^{1;1,1}_{0;1,2} = -\tfrac{17}{24}h^{-1}_{2,\delta}$$
$${}_{\delta,\frac{1}{2}}U^{1;1,1}_{0;1,3} = -\tfrac{3}{8}h^{-1}_{2,\delta}$$
$${}_{\delta,\frac{1}{2}}U^{1;1,1}_{0;1,4} = \tfrac{5}{24}h^{-1}_{2,\delta}$$
$${}_{\delta,\frac{1}{2}}U^{1;1,1}_{0;1,5} = -\tfrac{1}{24}h^{-1}_{2,\delta}$$

for $\delta = 1, \ldots, n$ with $h_{2,\delta} = h_2 \eta_{2,\delta}(\delta - 1, 0)$, and

$$
\begin{aligned}
{}_{\delta,1}U^{1;\underline{k},1}_{0;k,1} &= h_{2,\delta}^{-1} - \frac{h_{2,\delta}}{12}\left(\left(\eta^{-1}\frac{\partial \eta}{\partial x_2}\right)^2\right)^{k,\frac{3}{2}} - \left(\frac{\alpha}{12} - \frac{h_{2,\delta}^2}{24} a_0^{k,\frac{3}{2}}\right)\left(h_{2,\delta}^{-1} + \frac{1}{2}\left(\eta^{-1}\frac{\partial \eta}{\partial x_2}\right)^{k,\frac{3}{2}}\right), \\
{}_{\delta,1}U^{1;\underline{k},1}_{0;k-1,1} = {}_{\delta,1}U^{1;\underline{k},1}_{0;k+1,1} &= \frac{\alpha}{24}\left(h_{2,\delta}^{-1} + \frac{1}{2}\left(\eta^{-1}\frac{\partial \eta}{\partial x_2}\right)^{k,\frac{3}{2}}\right), \\
{}_{\delta,1}U^{1;\underline{k},1}_{0;k,2} &= -h_{2,\delta}^{-1} + \frac{h_{2,\delta}}{12}\left(\left(\eta^{-1}\frac{\partial \eta}{\partial x_2}\right)^2\right)^{k,\frac{3}{2}} + \left(\frac{\alpha}{12} - \frac{h_{2,\delta}^2}{24} a_0^{k,\frac{3}{2}}\right)\left(h_{2,\delta}^{-1} - \frac{1}{2}\left(\eta^{-1}\frac{\partial \eta}{\partial x_2}\right)^{k,\frac{3}{2}}\right), \\
{}_{\delta,1}U^{1;\underline{k},1}_{0;k-1,2} = {}_{\delta,1}U^{1;\underline{k},1}_{0;k+1,2} &= -\frac{\alpha}{24}\left(h_{2,\delta}^{-1} - \frac{1}{2}\left(\eta^{-1}\frac{\partial \eta}{\partial x_2}\right)^{k,\frac{3}{2}}\right),
\end{aligned}
$$

for $\delta = 1, \ldots, n$, $k = 1, \ldots, m_{1,\delta}$ with $\alpha = \left(\frac{h_{2,\delta}}{h_{0,\delta}}\right)^2$, $a_0^{k,\frac{3}{2}} = \kappa^2({}^{\delta,0}x_1^k, 0)$ under the proviso that

$$
\begin{aligned}
{}_{n,1}U^{1;m_{1,n},1}_{0;m_{1,n}+1,1} &= \frac{\alpha}{24}, \\
{}_{n,1}U^{1;m_{1,n},1}_{0;m_{1,n}+1,2} &= \frac{\alpha}{24}\left(\eta^{-1}\frac{\partial \eta}{\partial x_2}\right)^{m_{1,n},\frac{3}{2}}.
\end{aligned}
$$

Furthermore,

$$
\begin{aligned}
{}_{\delta,\frac{1}{2}}U^{1;1,m_2}_{0;1,m_2-4} &= -\tfrac{1}{24}h_{2,\delta}^{-1} \\
{}_{\delta,\frac{1}{2}}U^{1;1,m_2}_{0;1,m_2-3} &= \tfrac{5}{24}h_{2,\delta}^{-1} \\
{}_{\delta,\frac{1}{2}}U^{1;1,m_2}_{0;1,m_2-2} &= -\tfrac{3}{8}h_{2,\delta}^{-1} \\
{}_{\delta,\frac{1}{2}}U^{1;1,m_2}_{0;1,m_2-1} &= -\tfrac{17}{24}h_{2,\delta}^{-1} \\
{}_{\delta,\frac{1}{2}}U^{1;1,m_2}_{0;1,m_2} &= \tfrac{11}{12}h_{2,\delta}^{-1}
\end{aligned}
$$

for $\delta = 1, \ldots, n$ with $h_{2,\delta} = h_2 \eta_{2,\delta}(\delta - 1, 1)$, and

$$
\begin{aligned}
{}_{\delta,1}U^{1;\underline{k},m_2}_{0;k,m_2-1} =& - h_{2,\delta}^{-1} + \frac{h_{2,\delta}}{12}\left(\left(\eta^{-1}\frac{\partial \eta}{\partial x_2}\right)^2\right)^{k,m_2-\frac{1}{2}} \\
&+ \left(\frac{\alpha}{12} - \frac{h_{2,\delta}^2}{24} a_0^{k,m_2-\frac{1}{2}}\right)\left(h_{2,\delta}^{-1} + \frac{1}{2}\left(\eta^{-1}\frac{\partial \eta}{\partial x_2}\right)^{k,m_2-\frac{1}{2}}\right), \\
{}_{\delta,1}U^{1;\underline{k},m_2}_{0;k-1,m_2-1} =& {}_{\delta,1}U^{1;\underline{k},m_2}_{0;k+1,m_2-1} = -\frac{\alpha}{24}\left(h_{2,\delta}^{-1} + \frac{1}{2}\left(\eta^{-1}\frac{\partial \eta}{\partial x_2}\right)^{k,m_2-\frac{1}{2}}\right), \\
{}_{\delta,1}U^{1;\underline{k},m_2}_{0;k,m_2} =& h_{2,\delta}^{-1} - \frac{h_{2,\delta}}{12}\left(\left(\eta^{-1}\frac{\partial \eta}{\partial x_2}\right)^2\right)^{k,m_2-\frac{1}{2}} \\
&- \left(\frac{\alpha}{12} - \frac{h_{2,\delta}^2}{24} a_0^{k,m_2-\frac{1}{2}}\right)\left(h_{2,\delta}^{-1} - \frac{1}{2}\left(\eta^{-1}\frac{\partial \eta}{\partial x_2}\right)^{k,m_2-\frac{1}{2}}\right), \\
{}_{\delta,1}U^{1;\underline{k},m_2}_{0;k-1,m_2} =& {}_{\delta,1}U^{1;\underline{k},m_2}_{0;k+1,m_2} = \frac{\alpha}{24}\left(h_{2,\delta}^{-1} - \frac{1}{2}\left(\eta^{-1}\frac{\partial \eta}{\partial x_2}\right)^{k,m_2-\frac{1}{2}}\right),
\end{aligned}
$$

for $\delta = 1, \ldots, n$, $k = 1, \ldots, m_{1,\delta}$ with $\alpha = \left(\frac{h_{2,\delta}}{h_{1,\delta}}\right)^2$, $a_0^{k,m_2-\frac{1}{2}} = \kappa^2({}^{\delta,1}x_1^k, r^1)$ under the proviso that

$$
\begin{aligned}
{}_{n,1}U^{1;m_{1,n},m_2}_{0;m_{1,n}+1,m_2-1} &= -\frac{\alpha}{24}\Big(\eta^{-1}\frac{\partial\eta}{\partial x_2}\Big)^{m_{1,n},m_2-\frac{1}{2}},\\
{}_{n,1}U^{1;m_{1,n},m_2}_{0;m_{1,n}+1,m_2} &= \frac{\alpha}{24}.
\end{aligned}
$$

The components ${}_{\delta,\beta}U^{0;\ell,q}_{0;j,p}$ denote quadrature weights for modal subintegrals in the sense that

$$
\begin{aligned}
\int_0^{z^0_{n+1}} \frac{1}{\varrho}\psi^0_m(x_1)p(x_1,0)dx_1 \approx{}& \sum_{\ell=1}^{m_{1,\delta}} \widetilde{\psi}^0_m({}^{\delta,0}x_1^\ell)\,{}_{\delta,1}U^{0;\ell,1}_{0;j,p}\;{}^{\delta,1}v^{0;j,p}\\
&+ \widetilde{\psi}^0_m(z^0_\delta)\,{}_{\delta,\frac{1}{2}}U^{0;1,1}_{0;1,p}\;{}^{\delta,\frac{1}{2}}v^{0;1,p}\\
&+ \widetilde{\psi}^0_m(z^0_{n+1})\,{}_{n+1,0}U^{0;1,1}_{0;0,1}\;{}^{n+1,0}v^{0;0,1},\\
\int_0^{z^1_{n+1}} \frac{1}{\varrho}\psi^1_m(x_1)p(x_1,r^1)dx_1 \approx{}& \sum_{\ell=1}^{m_{1,\delta}} \widetilde{\psi}^1_m({}^{\delta,1}x_1^\ell)\,{}_{\delta,1}U^{0;\ell,m_2}_{0;j,p}\;{}^{\delta,1}v^{0;j,p}\\
&+ \widetilde{\psi}^1_m(z^1_\delta)\,{}_{\delta,\frac{1}{2}}U^{0;1,m_2}_{0;1,p}\;{}^{\delta,\frac{1}{2}}v^{0;1,p}\\
&+ \widetilde{\psi}^1_m(z^1_{n+1})\,{}_{n+1,1}U^{0;1,1}_{0;0,1}\;{}^{n+1,1}v^{0;0,1},
\end{aligned}
$$

where summations over $\delta = 1, \ldots, n$ are implied by the summation convention. The components of U for $e = 0$ are defined in two steps. Firstly, they are given as weights ${}_{\delta,\beta}\widetilde{U}^{0;k,q}_{0;j,p}$ intended for interpolation of $p(x_1, x_2)$ at the nodes on the vertical boundaries. By exploiting similar approximation techniques as for the case $e = 1$, we obtain the following interpolation weights

$$
\begin{aligned}
{}_{\delta,\frac{1}{2}}\widetilde{U}^{0;1,1}_{0;1,1} &= \frac{5}{16}, \quad {}_{\delta,\frac{1}{2}}\widetilde{U}^{0;1,1}_{0;1,2} = \frac{15}{16}, \quad {}_{\delta,\frac{1}{2}}\widetilde{U}^{0;1,1}_{0;1,3} = -\frac{5}{16}, \quad {}_{\delta,\frac{1}{2}}\widetilde{U}^{0;1,1}_{0;1,4} = \frac{1}{16},\\
{}_{\delta,1}\widetilde{U}^{0;1,1}_{0;1,1} &= \frac{1}{2} + \frac{\alpha}{8} + \frac{h_{2,\delta}^2}{16} a_0^{1,\frac{3}{2}} - \frac{h_{2,\delta}}{8}\Big(\eta^{-1}\frac{\partial \eta}{\partial x_2}\Big)^{1,\frac{3}{2}},\\
{}_{\delta,1}\widetilde{U}^{0;1,1}_{0;1,2} &= \frac{1}{2} + \frac{\alpha}{8} + \frac{h_{2,\delta}^2}{16} a_0^{1,\frac{3}{2}} + \frac{h_{2,\delta}}{8}\Big(\eta^{-1}\frac{\partial \eta}{\partial x_2}\Big)^{1,\frac{3}{2}},\\
{}_{\delta,1}\widetilde{U}^{0;1,1}_{0;2,p} &= -\frac{5\alpha}{16}, \quad {}_{\delta,1}\widetilde{U}^{0;1,1}_{0;3,p} = \frac{\alpha}{4}, \quad {}_{\delta,1}\widetilde{U}^{0;1,1}_{0;4,p} = -\frac{\alpha}{16},\\
{}_{\delta,1}\widetilde{U}^{0;\underline{k},1}_{0;k-1,p} &= \frac{\alpha}{16},\\
{}_{\delta,1}\widetilde{U}^{0;\underline{k},1}_{0;k,1} &= \frac{1}{2} - \frac{\alpha}{8} + \frac{h_{2,\delta}^2}{16} a_0^{k,\frac{3}{2}} - \frac{h_{2,\delta}}{8}\Big(\eta^{-1}\frac{\partial \eta}{\partial x_2}\Big)^{k,\frac{3}{2}},\\
{}_{\delta,1}\widetilde{U}^{0;\underline{k},1}_{0;k,2} &= \frac{1}{2} - \frac{\alpha}{8} + \frac{h_{2,\delta}^2}{16} a_0^{k,\frac{3}{2}} + \frac{h_{2,\delta}}{8}\Big(\eta^{-1}\frac{\partial \eta}{\partial x_2}\Big)^{k,\frac{3}{2}},\\
{}_{\delta,1}\widetilde{U}^{0;\underline{k},1}_{0;k+1,p} &= \frac{\alpha}{16},\\
{}_{\delta,1}\widetilde{U}^{0;m_{1,\delta},1}_{0;m_{1,\delta}-3,p} &= -\frac{\alpha}{16}, \quad {}_{\delta,1}\widetilde{U}^{0;m_{1,\delta},1}_{0;m_{1,\delta}-2,p} = \frac{\alpha}{4}, \quad {}_{\delta,1}\widetilde{U}^{0;m_{1,\delta},1}_{0;m_{1,\delta}-1,p} = -\frac{5\alpha}{16},\\
{}_{\delta,1}\widetilde{U}^{0;m_{1,\delta},1}_{0;m_{1,\delta},1} &= \frac{1}{2} + \frac{\alpha}{8} + \frac{h_{2,\delta}^2}{16} a_0^{m_{1,\delta},\frac{3}{2}} - \frac{h_{2,\delta}}{8}\Big(\eta^{-1}\frac{\partial \eta}{\partial x_2}\Big)^{m_{1,\delta},\frac{3}{2}},\\
{}_{\delta,1}\widetilde{U}^{0;m_{1,\delta},1}_{0;m_{1,\delta},2} &= \frac{1}{2} + \frac{\alpha}{8} + \frac{h_{2,\delta}^2}{16} a_0^{m_{1,\delta},\frac{3}{2}} + \frac{h_{2,\delta}}{8}\Big(\eta^{-1}\frac{\partial \eta}{\partial x_2}\Big)^{m_{1,\delta},\frac{3}{2}},
\end{aligned}
$$

for $\delta = 1, \ldots, n$, $k = 2, \ldots, m_{1,\delta} - 1$, $p = 1, 2$ with $h_{2,\delta} = h_2 \eta_{2,\delta}(\delta - 1, 0)$, $\alpha = \big(\frac{h_{2,\delta}}{h_{0,\delta}}\big)^2$, $a_0^{k,\frac{3}{2}} = \kappa^2({}^{\delta,0}x_1^k, 0)$.

Furthermore,

$$
{}_{\delta,\frac{1}{2}}\widetilde{U}^{0;1,m_2}_{0;1,m_2-3} = \frac{1}{16}, \quad {}_{\delta,\frac{1}{2}}\widetilde{U}^{0;1,m_2}_{0;1,m_2-2} = -\frac{5}{16}, \quad {}_{\delta,\frac{1}{2}}\widetilde{U}^{0;1,m_2}_{0;1,m_2-1} = \frac{15}{16}, \quad {}_{\delta,\frac{1}{2}}\widetilde{U}^{0;1,m_2}_{0;1,m_2} = \frac{5}{16},
$$

$$
\begin{aligned}
{}_{\delta,1}\widetilde{U}^{0;1,m_2}_{0;1,m_2-1} &= \frac{1}{2} + \frac{\alpha}{8} + \frac{h_{2,\delta}^2}{16} a_0^{1,m_2-\frac{1}{2}} - \frac{h_{2,\delta}}{8}\Big(\eta^{-1}\frac{\partial\eta}{\partial x_2}\Big)^{1,m_2-\frac{1}{2}}, \\
{}_{\delta,1}\widetilde{U}^{0;1,m_2}_{0;1,m_2} &= \frac{1}{2} + \frac{\alpha}{8} + \frac{h_{2,\delta}^2}{16} a_0^{1,m_2-\frac{1}{2}} + \frac{h_{2,\delta}}{8}\Big(\eta^{-1}\frac{\partial\eta}{\partial x_2}\Big)^{1,m_2-\frac{1}{2}}, \\
{}_{\delta,1}\widetilde{U}^{0;1,m_2}_{0,2,p} &= -\frac{5\alpha}{16}, \quad {}_{\delta,1}\widetilde{U}^{0;1,m_2}_{0,3,p} = \frac{\alpha}{4}, \quad {}_{\delta,1}\widetilde{U}^{0;1,m_2}_{0,4,p} = -\frac{\alpha}{16}, \\
{}_{\delta,1}\widetilde{U}^{0;\underline{k},m_2}_{0;k-1,p} &= \frac{\alpha}{16}, \\
{}_{\delta,1}\widetilde{U}^{0;\underline{k},m_2}_{0;k,m_2-1} &= \frac{1}{2} - \frac{\alpha}{8} + \frac{h_{2,\delta}^2}{16} a_0^{k,m_2-\frac{1}{2}} - \frac{h_{2,\delta}}{8}\Big(\eta^{-1}\frac{\partial\eta}{\partial x_2}\Big)^{k,m_2-\frac{1}{2}}, \\
{}_{\delta,1}\widetilde{U}^{0;\underline{k},m_2}_{0;k,m_2} &= \frac{1}{2} - \frac{\alpha}{8} + \frac{h_{2,\delta}^2}{16} a_0^{k,m_2-\frac{1}{2}} + \frac{h_{2,\delta}}{8}\Big(\eta^{-1}\frac{\partial\eta}{\partial x_2}\Big)^{k,m_2-\frac{1}{2}}, \\
{}_{\delta,1}\widetilde{U}^{0;\underline{k},m_2}_{0;k+1,p} &= \frac{\alpha}{16}, \\
{}_{\delta,1}\widetilde{U}^{0;m_{1,\delta},m_2}_{0;m_{1,\delta}-3,p} &= -\frac{\alpha}{16}, \quad {}_{\delta,1}\widetilde{U}^{0;m_{1,\delta},m_2}_{0;m_{1,\delta}-2,p} = \frac{\alpha}{4}, \quad {}_{\delta,1}\widetilde{U}^{0;m_{1,\delta},m_2}_{0;m_{1,\delta}-1,p} = -\frac{5\alpha}{16}, \\
{}_{\delta,1}\widetilde{U}^{0;m_{1,\delta},m_2}_{0;m_{1,\delta},m_2-1} &= \frac{1}{2} + \frac{\alpha}{8} + \frac{h_{2,\delta}^2}{16} a_0^{m_{1,\delta},m_2-\frac{1}{2}} - \frac{h_{2,\delta}}{8}\Big(\eta^{-1}\frac{\partial\eta}{\partial x_2}\Big)^{m_{1,\delta},m_2-\frac{1}{2}}, \\
{}_{\delta,1}\widetilde{U}^{0;m_{1,\delta},m_2}_{0;m_{1,\delta},m_2} &= \frac{1}{2} + \frac{\alpha}{8} + \frac{h_{2,\delta}^2}{16} a_0^{m_{1,\delta},m_2-\frac{1}{2}} + \frac{h_{2,\delta}}{8}\Big(\eta^{-1}\frac{\partial\eta}{\partial x_2}\Big)^{m_{1,\delta},m_2-\frac{1}{2}},
\end{aligned}
$$

for $\delta = 1, \ldots, n$, $k = 2, \ldots, m_{1,\delta} - 1$, $p = m_2 - 1, m_2$ with $h_{2,\delta} = h_2\eta_{2,\delta}(\delta - 1, 1)$, $\alpha = \big(\frac{h_{2,\delta}}{h_{1,\delta}}\big)^2$, $a_0^{k,m_2-\frac{1}{2}} = \kappa^2({}^{\delta,1}x_1^k, r^1)$.

Secondly, the interpolation weights are scaled into quadrature weights. Assuming that $m_{1,\delta}$ is odd, the use of the composite Simpson's rule yields the following scaling

$$
\begin{aligned}
{}_{1,\frac{1}{2}}U^{0;1,1}_{0;1,p} &= \frac{1}{3}\frac{h_{0,1}}{\varrho_1}\, {}_{1,\frac{1}{2}}\widetilde{U}^{0;1,1}_{0;1,p}, \\
{}_{1,\frac{1}{2}}U^{0;1,m_2}_{0;1,p} &= \frac{1}{3}\frac{h_{1,1}}{\varrho_1}\, {}_{1,\frac{1}{2}}\widetilde{U}^{0;1,m_2}_{0;1,p}, \\
{}_{\delta,\frac{1}{2}}U^{0;1,1}_{0;1,p} &= \frac{1}{3}\Big(\frac{h_{0,\delta-1}}{\varrho_{\delta-1}} + \frac{h_{0,\delta}}{\varrho_\delta}\Big)\, {}_{\delta,\frac{1}{2}}\widetilde{U}^{0;1,1}_{0;1,p} \\
{}_{\delta,\frac{1}{2}}U^{0;1,m_2}_{0;1,p} &= \frac{1}{3}\Big(\frac{h_{1,\delta-1}}{\varrho_{\delta-1}} + \frac{h_{1,\delta}}{\varrho_\delta}\Big)\, {}_{\delta,\frac{1}{2}}\widetilde{U}^{0;1,m_2}_{0;1,p}, \quad \delta = 2, \ldots, n, \\
{}_{n+1,0}U^{0;1,1}_{0;0,1} &= \frac{1}{3}\frac{h_{0,n}}{\varrho_n}, \\
{}_{n+1,1}U^{0;1,1}_{0;0,1} &= \frac{1}{3}\frac{h_{1,n}}{\varrho_n},
\end{aligned}
$$

and for $\delta = 1, \dots, n$,

$$\left.\begin{aligned} {}_{\delta,1}U^{0;\ell,1}_{0;j,p} &= \frac{4}{3}\frac{h_{0,\delta}}{\varrho_\delta}\,{}_{\delta,1}\widetilde{U}^{0;\ell,1}_{0;j,p} \\ {}_{\delta,1}U^{0;\ell,m_2}_{0;j,p} &= \frac{4}{3}\frac{h_{1,\delta}}{\varrho_\delta}\,{}_{\delta,1}\widetilde{U}^{0;\ell,m_2}_{0;j,p} \end{aligned}\right\}, \quad \ell = 1, 3, \dots, m_{1,\delta},$$

$$\left.\begin{aligned} {}_{\delta,1}U^{0;\ell,1}_{0;j,p} &= \frac{2}{3}\frac{h_{0,\delta}}{\varrho_\delta}\,{}_{\delta,1}\widetilde{U}^{0;\ell,1}_{0;j,p} \\ {}_{\delta,1}U^{0;\ell,m_2}_{0;j,p} &= \frac{2}{3}\frac{h_{1,\delta}}{\varrho_\delta}\,{}_{\delta,1}\widetilde{U}^{0;\ell,m_2}_{0;j,p} \end{aligned}\right\}, \quad \ell = 2, 4, \dots, m_{1,\delta} - 1.$$

Acknowledgments

The authors express their gratitude to Dr. Elisabeth Larsson for her interest and support of this work, and for her constructive advice.

References

[1] K. Åhlander and K. Otto, *Software design for finite difference schemes based on index notation*, Future Generation Comput. Syst., 22 (2006), pp. 102–109.

[2] L. M. Brekhovskikh and O. A. Godin, *Acoustics of Layered Media I*, Springer-Verlag, Berlin, 1990.

[3] A. J. Burton and G. F. Miller, *The application of integral equation methods to the numerical solution of some exterior boundary-value problems*, Proc. Roy. Soc. London Ser. A, 323 (1971), pp. 201–210.

[4] L. Collatz, *The Numerical Treatment of Differential Equations*, Springer-Verlag, Berlin, 3rd ed., 1960.

[5] P. J. Davis and P. Rabinowitz, *Methods of Numerical Integration*, Academic Press, San Diego, CA, 2nd ed., 1984.

[6] G. J. Fix and S. P. Marin, *Variational methods for underwater acoustic problems*, J. Comput. Phys., 28 (1978), pp. 253–270.

[7] L. Gaul, M. Kögl, and M. Wagner, *Boundary Element Methods for Engineers and Scientists*, Springer-Verlag, Berlin, 2003.

[8] F. B. Jensen, W. A. Kuperman, M. B. Porter, and H. Schmidt, *Computational Ocean Acoustics*, AIP Press, New York, 1994.

[9] J. B. Keller and D. Givoli, *Exact non-reflecting boundary conditions*, J. Comput. Phys., 82 (1989), pp. 172–192.

[10] P. Knupp and S. Steinberg, *Fundamentals of Grid Generation*, CRC Press, Boca Raton, FL, 1993.

[11] J. C. Lachat and J. O. Watson, *Effective numerical treatment of boundary integral equations: A formulation for three-dimensional elastostatics*, Int. J. Numer. Methods Engrg., 10 (1976), pp. 991–1005.

[12] E. Larsson, *A domain decomposition method for the Helmholtz equation in a multilayer domain*, SIAM J. Sci. Comput., 20 (1999), pp. 1713–1731.

[13] E. Larsson and L. Abrahamsson, *Helmholtz and parabolic equation solutions to a benchmark problem in ocean acoustics*, J. Acoust. Soc. Amer., 113 (2003), pp. 2446–2454.

[14] P. M. Morse and H. Feshbach, *Methods of Theoretical Physics*, McGraw–Hill, New York, 1953.

[15] K. Otto, *Iterative solution of the Helmholtz equation by a fourth-order method*, in suppl, vol. 40:1 of Boll. Geof. Teor. Appl., 1999, pp. 104–105.

[16] ——, *A unifying framework for preconditioners based on fast transforms*, Report 187 (revised), Dept. of Scientific Computing, Uppsala Univ., Uppsala, Sweden, 1999.

[17] K. Otto and E. Larsson, *Iterative solution of the Helmholtz equation by a second-order method*, SIAM J. Matrix Anal. Appl., 21 (1999), pp. 209–229.

[18] J. G. Papastavridis, *Tensor Calculus and Analytical Dynamics*, CRC Press, Boca Raton, FL, 1999.

[19] A. F. Peterson, S. L. Ray, and R. Mittra, *Computational Methods for Electromagnetics*, IEEE Press, New York, 1998.

[20] H. A. Schenck, *Improved integral formulation for acoustic radiation problems*, J. Acoust. Soc. Amer., 44 (1968), pp. 41–58.

[21] A. H. Stroud and D. Secrest, *Gaussian Quadrature Formulas*, Prentice–Hall, Englewood Cliffs, NJ, 1966.

[22] V. V. Varadan, A. Lakhtakia, and V. K. Varadan, eds., *Acoustic, Electromagnetic, and Elastic Wave Scattering*, vol. 1, Elsevier Science Publishers, Amsterdam, The Netherlands, 1991.